9-14-2017

Effect of Fused Filament Fabrication Process Parameters on the Mechanical Properties of Carbon Fiber Reinforced Polymers

Abdulrahman S. Alwabel

EFFECT OF FUSED FILAMENT FABRICATION PROCESS PARAMETERS ON THE MECHANICAL PROPERTIES OF CARBON FIBER REINFORCED POLYMERS

THESIS

Abdulrahman S. Alwabel,1st Lt, RSAF

AFIT-ENV-MS-17-S-046

DEPARTMENT OF THE AIR FORCE
AIR UNIVERSITY

AIR FORCE INSTITUTE OF TECHNOLOGY

Wright-Patterson Air Force Base, Ohio

The views expressed in this document are those of the author and do not reflect the official policy or position of the United States Air Force, the Department of Defense, the United States Government, the Royal Saudi Air Force, the Kingdom of Saudi Arabia Government, or any other defense organization.

AFIT-ENV-MS-17-S-046

EFFECT OF FUSED FILAMENT FABRICATION PROCESS PARAMETERS ON THE MECHANICAL PROPERTIES OF CARBON FIBER REINFORCED POLYMERS

THESIS

Presented to the Faculty

Department of Systems Engineering and Management

Graduate School of Engineering and Management

Air Force Institute of Technology

Air University

Air Education and Training Command

In Partial Fulfillment of the Requirements for the

Degree of Master of Science in Engineering Management

Abdulrahman S. Alwabel, BS

1st Lt, RSAF

September 2017

EFFECT OF FUSED FILAMENT FABRICATION PROCESS PARAMETERS ON THE MECHANICAL PROPERTIES OF CARBON FIBER REINFORCED POLYMERS

Abdulrahman S. Alwabel, BS
1st Lt, RSAF

Committee Membership:

Maj Jason K. Freels, PhD
Chair

Maj Ryan P. O'Hara, PhD
Member

Dr. Heather J. Chaput, PhD
External Member

Abstract

Carbon fiber reinforced polymer manufactured using additive manufacturing process is relatively a new process. The ability to predict the mechanical properties of these parts with high confidence will spread the use of these high-strength materials in more applications. The purpose of this research was to determine the effect of the build time between successive layers, arrangement of fiber and nylon layers, fiber start location, and the use of support material on the mechanical properties CFRP produced by additive manufacturing process using the MarkForged (MarkOne) 3D printer. A design of experiment (DOE) we preformed to develop a mathematical model describing the functional relationship between the tensile strength of additively manufactured composites and the selected additive manufacturing build process parameters. Testing was performed in accordance with ASTM standard D3039 using the 25 manufactured specimens. The mechanical properties were measured in the experiment were tensile strength, and tensile stress. A liner regression analysis was preformed to determine the relation between the ultimate tensile strength and the main level interactions of the four build parameters. The results showed a significant positive relation longer the build time between successive layers, and negative relation with the other fiber and nylon layer arrangement. However, the two other build parameters showed negative, but not significant results.

Acknowledgment

I would first like to thank my thesis advisor, Major Jason K. Freels. The door to Major Freels office was always open whenever I ran into a trouble spot or had a question about my research or writing. He consistently allowed this paper to be my own work, but steered me in the right the direction whenever he thought I needed it. I would also like to acknowledge Major Ryan P. O'Hara from the Department of Aeronautics & Astronautics, Aeronautical Engineering, and Dr. Heather J. Chaput from the Air Force Research Lab for guiding my research and for their very valuable comments on this thesis.

Finally, I must express my very profound gratitude to my parents, family, and friends for providing me with unfailing support and continuous encouragement throughout my years of study and through the process of researching and writing this thesis. This accomplishment would not have been possible without them. Thank you.

Abdulrahman S. Alwabel

Table of Contents

List of Figures

List of Tables

EFFECT OF FUSED FILAMENT FABRICATED PROCESS PARAMETERS ON THE MECHANICAL PROPERTIES OF CARBON FIBER REINFORCED POLYMERS

I. Introduction

Background

Since the industrial revolution, many new manufacturing methods have been introduced – each promising to deliver cheaper products with improved properties. However, with the introduction of each new method, comes the challenge of optimizing the build process parameters to ensure that the properties of the resulting products are consistent and reliable. Such improvements occur in different forms, some directly impact the part by improving the output properties or quality, while other improvements are indirect, such as reducing waste during the manufacturing process.

Additive manufacturing (AM) is relatively new manufacturing process that allows for the creation of objects with highly complex geometries that would otherwise be difficult to produce using the traditional methods. AM is most often referred to as "3D printing", however there are four distinct additive manufacturing processes: liquid polymer systems, discrete particle systems, molten material systems, and solid sheet systems (Gibson, Rosen, & Stucker, 2014). AM was created in 1984 when three parallel patents were filed describing the same concept of fabricating objects in three dimensions. Since that time the use of AM has grown rapidly with an increasing number of material options and the capability to produce parts that are custom-fit for each consumer's requirements – without the need to change the production line.

AM utilizes three-dimensional computer-aided design (CAD) models to create an object by selectively adding material. This process allows for significantly less part production waste

compared to ‘subtractive’ manufacturing methods such as Computer Numeric Control (CNC) machining. However, AM is not currently as mature as traditional manufacturing methods with respect to the time required to manufacture and the ability to deliver products with consistent mechanical properties.

This research investigates the effect of changing several AM build process parameters on the mechanical properties of unidirectional carbon fiber reinforced polymer (CFRP) manufactured using the MarkForged® MarkOne 3D printer. The parameters chosen for this research are limited to what the user could control in the MarkOne CFRP manufacturing process. The goal of this investigation is to determine which combinations of AM build process parameters produce CFRP specimens with the highest tensile strength. Due to FRP’s strength and relatively lightweight it became a critical part of today’s advance engineering. They are used in the aerospace industry, automotive, civil construction, and sporting goods along with many more. By merging the capabilities of additive manufacturing and the properties of FRP’s, it opens new potentials from prototyping to more custom products in the medical failed and small-scale businesses.

Traditional manufactured CFRP is relatively mature process with decades of research on the manufacturing parameters effecting the parts mechanical properties. On the other hand, AM just began exploring the ability to produce CFRP using existing and new AM technologies. Due to the relatively undeveloped field and the differences in the manufacturing processes, research must explore which build parameters significantly impact the mechanical strength of CFRP parts produced using AM. There are many possible parameters that could be explored from the type of AM process to the specifics like manufacturing conditions.

The MarkOne 3D printer printing heads with two processes; Continuous Filament Fabrication (CFF) and Fused Filament Fabrication (FFF) (MarkForged Inc., 2015). FFF and CFF are the process of extruding the material from a heated extrusion head that is moving in a plane parallel to the build surface or plate. The thermoplastic melts and passes through the extraction nozzle to be deposited into the build surface with the desired x-y shape. When the layer is finished the print bed is lowered and the process repeats until the desired 3D shape is completed (Gibson et al., 2014).

Research Approach

This research investigates the impact that several Fused Filament Fabrication (FFF) process parameters have on the ultimate tensile strength of CFRP specimens produced using the MarkForged® MarkOne printer. The test points included in this research will allow estimation of the effect of one and two-level interactions between four factors: layer height, fiber start location, time between layers, and fiber arrangement. The specimens to be manufactured in 250 mm × 15mm × 3mm in length, width, and thickness respectively with the four different parameters. Prior to testing, manufacturing conditions were recorded and each specimen's dimension measured. Tensile tests were conducted per ASTM D3039 using five specimens per test point on MTS 810 Material Test System. A statistical analysis was performed to determine which factors had a statistically significant effect on the ultimate tensile strength.

Limitation of the Current AM CFRP

Due to the difference in manufacturing processes, this presents several challenges to the current CFRP. Part strength and mass production time among many other limitations limit the spreading of this technology in mass production markets. According to the MarkForged® Data sheet for the MarkOne printer, mechanical properties carbon fiber tensile strength is 700Mpa

(MarkForged Inc., 2015). On the other hand, traditional manufactured unidirectional CFRP with fiber content of approximately 50% of the volume typically has a tensile strength of 1000Mpa (Callister, 2007). Moreover, using AM to produce large scale high-strength parts is limited due to the possible distortion caused by thermal gradients in the part during the manufacturing process (Love et al., 2014). Composite materials can be affected by many factors; high and low temperatures, humidity, water expositor, and many other operational condition, which require the behavior of the material to be studied thoroughly under the exposure conditions that are likely to be experienced.

Research Objective

The objective of this research is to determine the effect of different process parameters on the tensile strength properties of CFRP produced by additive manufacturing process using the MarkForged (MarkOne) 3D printer. The results of this research effort and that of future follow-up research efforts may help to produce reliable, high strength parts that meet the specifications of traditionally manufactured parts or determine the difference in capabilities and factors effecting additive manufacturing.

Document Overview

This document is organized using a standard five-chapter thesis format. Following this introduction, Chapter II summarizes the literature used to accomplish this research. Chapter II will review design of experiment full factorial and fractional factorial designs. Chapter II also includes a review of the failure mechanics of unidirectional composites. Finally, in Chapter II the process and parameters used by the MarkOne 3D printer are explored.

Chapter III describes the manufacturing and testing procedures used in this study. Chapter III also includes the different observed manufacturing inconsistencies and issues.

Chapter III summarizes statistical analysis and the calculations used to obtain the mechanical properties. Chapter IV shows the results obtained from the tensile test and the liner regression analysis, as well as the model validation. Chapter V is a summary of this research effort and discusses future research recommendations.

II. Literature Review

Chapter Overview

This chapter summarizes information found in the literature that was used in the progress of this research. First, a review of experimental designs is presented, emphasizing the differences between full-factorial and fractional factorial designs. Next, the failure mechanics for traditionally manufactured unidirectional composites is reviewed. Finally, the process and parameters used by the MarkOne 3D printer are explored. Starting with the process of importing the computer-aided design (CAD) into the slicing software (Eiger); then explaining the factors that affect the process of manufacturing CFRP which are controlled within the software.

Design of Experiment (DOE)

DOE is a method to determine the relationship between different parameters affecting the experiment output using a minimized number of experiments. The reason for designing an experiment is to obtain the major interest at lower cost. There are different factorial designs ranging from full factorial to different fractional factorials. Fractional factorial was introduced and used by Fisher in 1942 in agricultural experiments (Stewart, 2005). Although, testing the full factorial is the more comprehensive test, sometimes this is not feasible. People usually refer to fractional factorial because of the simplicity it provides. This might potentially cause the loss of important interactions, but will reduce cost, time, and overall logistics. Let us consider an experiment using four design factors A, B, and C with each factor using two levels; this will result in 8 different test points when considering the full factorial design (Table 1). On the other hand, using half fractional factorial design will reduce the number of test points to 4 (

Table 2). By using half fractional factorial, the experimenter would face less logistical problems. However, since there is less data points a decision must be made on studying a two-way interaction or studying the main effects.

Table 1. Three Factor, Two Level Full Factroial Design

Test Point	Factor A	Factor B	Factor C
1	-	-	-
2	+	-	-
3	-	+	-
4	+	+	-
5	-	-	+
6	+	-	+
7	-	+	+
8	+	+	+

Table 2. Three Factor, Two Level Half Fractional Factorial Design

Test Point	Factor A	Factor B	Factor C
1	-	-	-
2	+	-	-
3	-	+	-
4	+	+	-
5	-	-	+
6	+	-	+
7	-	+	+
8	+	+	+

1st Half Factorial
2nd Half Factorial

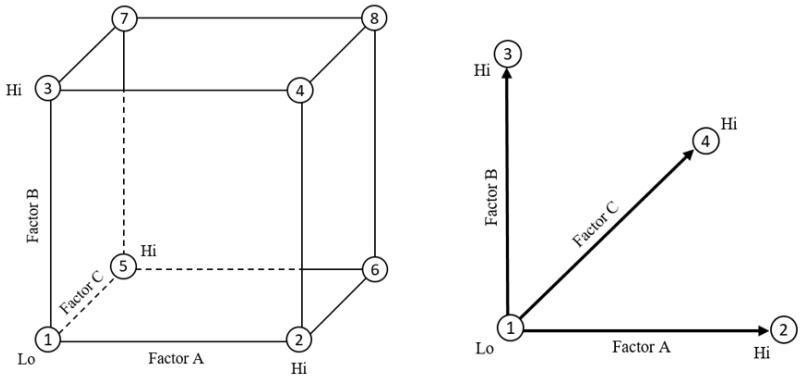

Figure 1. Comparison Between Full Factorial on the Right, Fractional Factorial on the Left (Anderson & Whitcomb, 2007)

Studying main effects only or what is called the single factor or one at a time can be achieved by controlling the other conditions except the one factor which to be investigated (Fisher, 1971). Fisher emphasize that we most likely cannot insure that any factor will exert its effects independently of the other factors; these potential interactions must be considered. However, sometimes testing all the factors simultaneously would be troubling or costly which leads the experimenter to use the one at a time method.

There are four categories of variables depending on the category in which the variable is assigned. First, primary variables are the variables of which main response performance can be effected and are thought of as primary interest. Second, background variables are variables that cannot or should not be constant in the experiment, they are often referred to as “noise”. These factors can be blocked to minimize the effect of day to day or operator to operator difference on the data using randomized block deign. Third, uncontrolled variables are variables that can or may not be identified but affect the experiment results. To ensure that these variables do not introduce bias into the results, randomization can be used. Finally, constant variables that should

be held constant in the experiment to minimize the experiment complexity. (Anderson & Whitcomb, 2007)

Carbon Fiber Reinforced Polymer

Carbon fiber began in 1879 with a patent by Edison for using carbon filaments in electric lamps. It is manufactured with dimeters ranging from 9 to 17 μm and then wounded into larger threads. (Masuelli, 2013)

"Fiber-Reinforced Polymer (FRP), also called Fiber-Reinforced Plastic, is a composite material made of a polymer matrix reinforced with fibers" (Masuelli, 2013). Fibers are usually Glass, Carbon, and/or Kevlar, although there are many more less common fibers been used. This research is meanly focused on Carbon Fiber Reinforced Plastic (CFP) which has a high strength to weight ratio, it is also referred to as Carbon Fiber Reinforced Polymer (CFRP) or Carbon Fiber Reinforced Thermoplastic (CFRTP).

FRP consists of two components reinforcement and the matrix. In the case of CFRP, the reinforcement is carbon fiber and the matrix is polymer. The structure contains lamina which is a plane of layer, and the laminate which is two or more laminae. Fiber lamina configurations could be unidirectional fiber or woven fabric; and the laminate could be unidirectional or multidirectional. The matrix role is to provide support and transfer local loads from one fiber to the other (Callister, 2007).

Generally, in the case of FRP the mechanical characteristics depend on the fiber properties and the rate of which the applied force is transferred from the matrix to the fiber. The load transfer between the matrix and the fiber results in deformation to the matrix (Figure 2) (Callister, 2007).

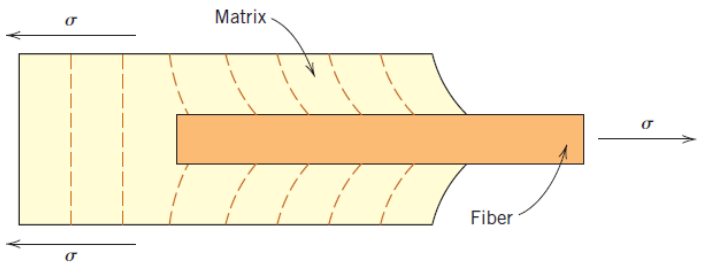

Figure 2. Matrix Deformation Surrounding Unidirectional Composite Under Longitudinal Tensile Loading (Callister, 2007)

In the case of unidirectional lamina longitudinal tension, the composite will fail when the longitudinal strain of either the fiber or the matrix reaches the ultimate tensile strain; in most cases the fiber strain is lower than matrix strain (Figure 3).

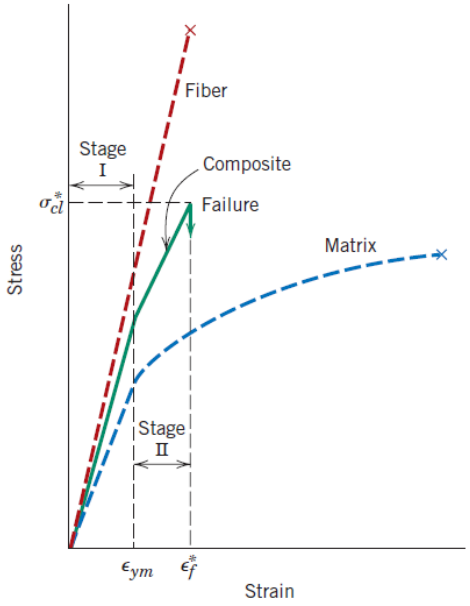

Figure 3. Typical Composite Failure Stress Strain Curve Under Longitudinal Tensile Loading (Callister, 2007)

In fiber dominated strength structures, fiber strength is different from each single fiber and point to the other. The fibers do not fail at the same time but isolated fibers break at weak points. This results in a nonuniform stress development around the broken fiber and an

interfacial shear stress with a high near the break location. The broken fiber stress transmutation is zero at the break point and gradually increases the further from the break (Figure 4). Single fiber break can take one of three forms shown in (Figure 5) with (a) Transverse Matrix Cracking for Brittle Matrix and Relatively Strong Interface, (b) Fiber/Matrix Debonding for Relatively Weak Interface and/or Relatively High Fiber Ultimate Strain, and (c) Conical Shear Fractures in Relatively Ductile Matrix and Strong Interface.

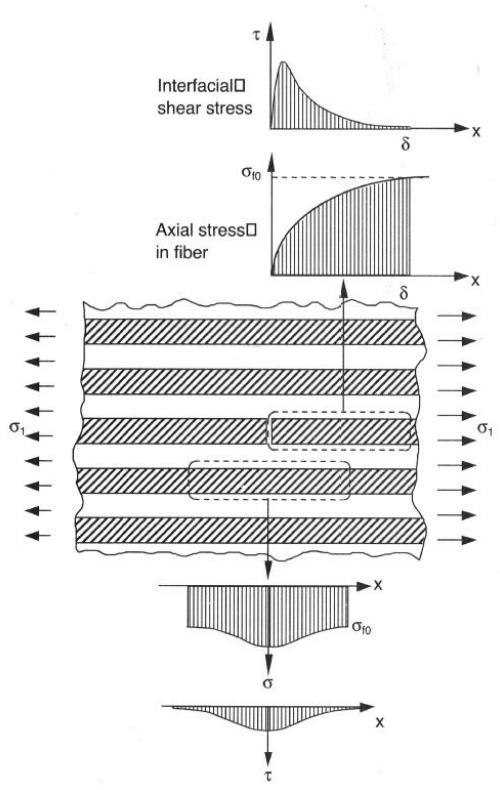

Figure 4. Local Stress Distribution Around Fiber Break in a Unidirectional Composite Under Longitudinal Tensile Loading (Daniel & Ishai, 2006)

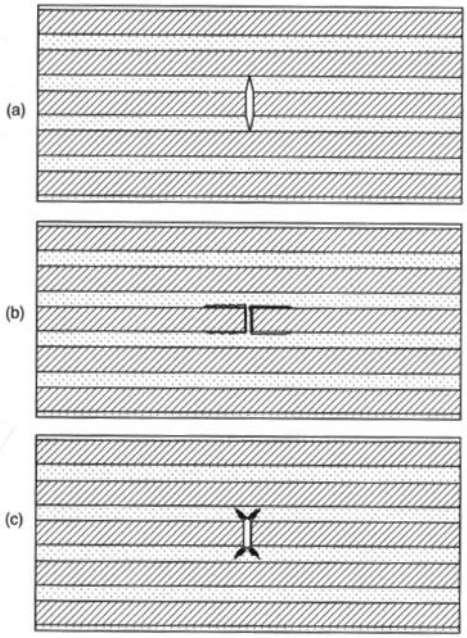

Figure 5. Single Fiber Failure Mechanisms in a Unidirectional Composite Under Longitudinal Tensile Loading (a) Transverse Matrix Cracking for Brittle Matrix and Relatively Strong Interface, (b) Fiber/Matrix Debonding for Relatively Weak Interface and/or Relatively High Fiber Ultimate Strain, and (c) Conical Shear Fractures in Relatively Ductile Matrix and Strong Interface (Daniel & Ishai, 2006)

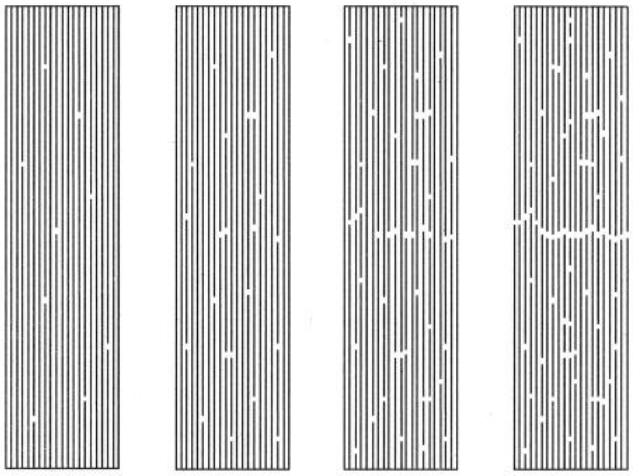

Figure 6. Unidirectional Composite Failure Sequence Under Longitudinal Tensile Loading (Daniel & Ishai, 2006)

MarkOne CFRP AM Manufacturing Process

MarkForged Inc. first introduced the MarkOne 3D printer in 2014, which is capable of printing continuous carbon fiber (CF), Kevlar, and fiberglass. The printer uses two print heads (extrusion nozzles) to create nylon parts with continuous fiber filaments; a patent pending Continuous Filament Fabrication (CFF) and a Fused Filament Fabrication (FFF) (MarkForged Inc., 2015). The nylon extrusion nozzle is heated and nylon will pass through creating the desired layer. On the other hand, carbon fiber is coated with a thermoplastic resin to create the extrusion filament. When the CF passes through the heated nozzle which melts the resin and fiber/risen bounds to the existing layer (Holm, 2016).

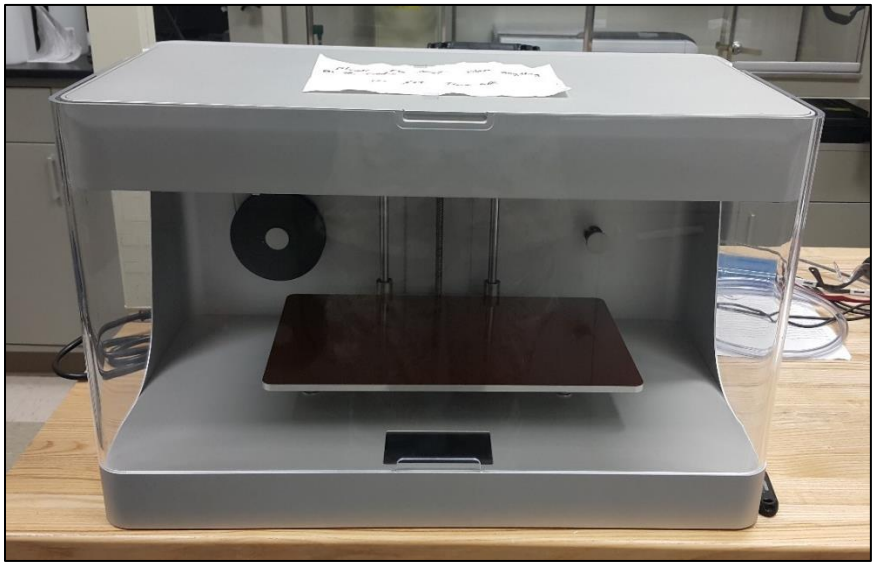

Figure 7. MarkOne 3D Printer

Figure 8. MarkOne 3D Printer Nylon Dry Box

The process starts with designing the part using a computer edit design (CAD) software. The CAD is then exported into a stereo-lithography formatted file and imported into Eiger® software which is web-based application developed by MarkForged. Eiger® is used as an interface for the printer in which the user can control the print parameters. The controllable manufacturing factors are layer height, fill pattern, fill density, number of fiber/nylon layers, fiber start location, and the use of supports or brim among many others. In this research, all factors will be fixed except fiber/nylon layers, fiber start location, and the use of supports along with time between layers.

First, layer height can be adjusted between 0.1-0.2mm with 0.01mm increments. However, it is only possible to change the layer height if the part will be nylon only otherwise it is fixed depending on the used fiber. CF uses a layer height of 0.125mm, Kevlar and fiberglass use 0.1mm.

Second, fill pattern for nylon there are three options rectangular, triangular, and hexagonal; in this research, only rectangular fill will be used (Figure 9). The rectangular fill uses

a (±45˚) placement relative to the print bed. On the other hand, fiber three options are concentric, isotropic, and full fill; however, for CF only concentric fill can be used (Figure 10). The CF concentric fill has a minimum continuous fiber length of 610mm per fiber cut due to the distance between the print head and the fiber cutter (MarkForged Inc., 2015).

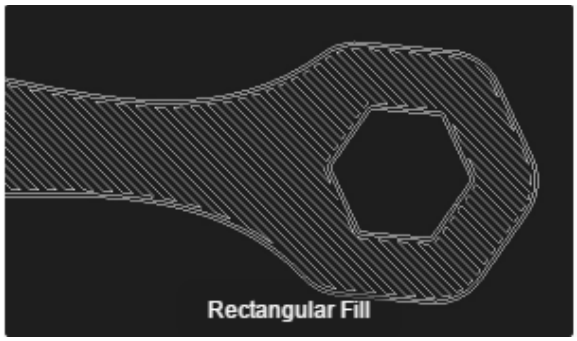

Figure 9. Screen Capture Illustrating Rectangular Plastic Fill Pattern ("Eiger," 2016)

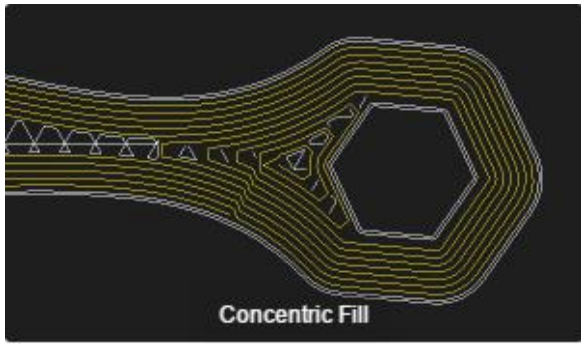

Figure 10. Screen Capture Illustrating Concentric Fiber Fill Pattern ("Eiger," 2016)

The fill density for nylon controls the density of the internal structure which can be adjusted up to 100%. A 100% fill creates a nearly solid plastic part or it can be lowered to create a fill pattern with less structural material. In this research, all nylon layer densities are fixed to 100%. Figure 11 through Figure 13 graphically depict items produced with various fill densities. For carbon fiber, concentric fiber rings are used to determine the fiber fill per layer. The maximum number of concentric fiber rings varies depending on the area available for fiber in

each layer. Figure 14 and Figure 15 show the effect of the number of concentric fiber rings on the fiber fill per layer.

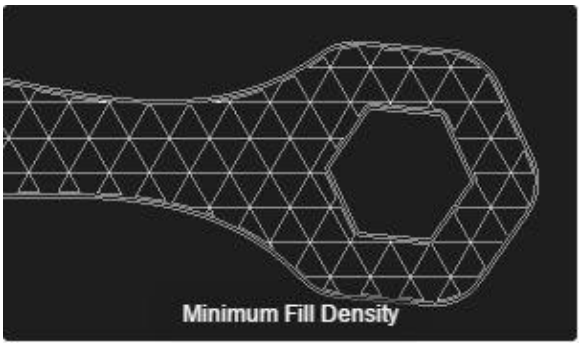

Figure 11. Screen Capture Illustrating Minimum Nylon Fill Density ("Eiger," 2016)

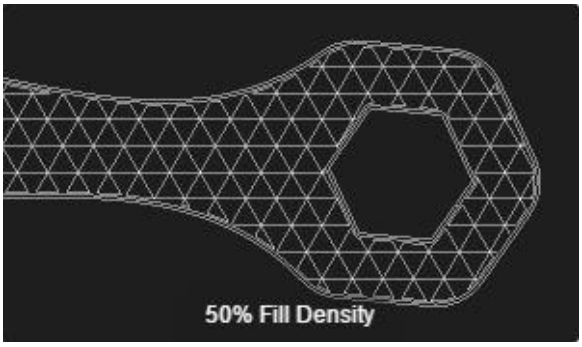

Figure 12. Screen Capture Illustrating 50% Nylon Fill Density ("Eiger," 2016)

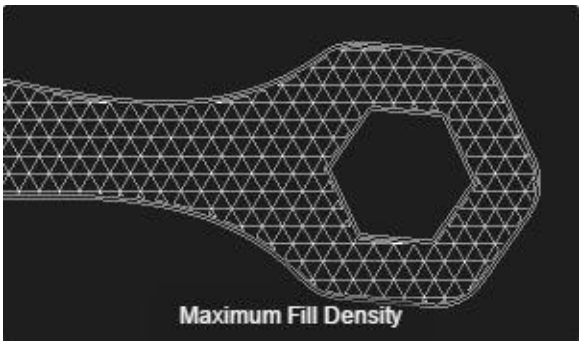

Figure 13. Screen Capture Illustrating Maximum Nylon Fill Density ("Eiger," 2016)

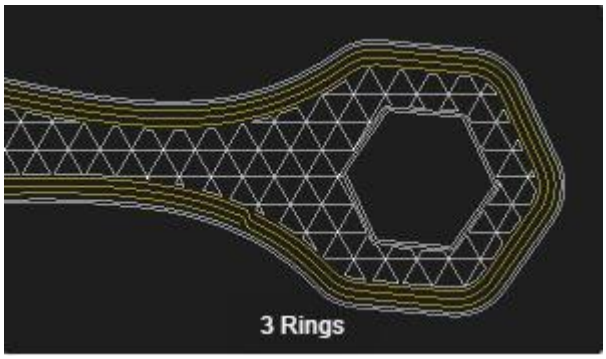

Figure 14. Screen Capture Illustrating Part with 3 Fiber Concentric Circles ("Eiger," 2016)

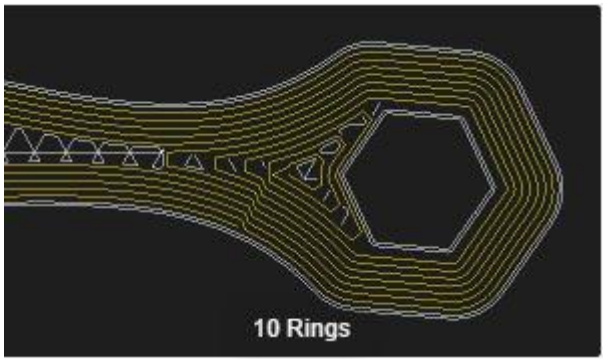

Figure 15. Screen Capture Illustrating Part with 10 Fiber Concentric Circles ("Eiger," 2016)

Users can also set the number of layers used for the side walls as well as the number layers used for the roof and floor layers. Figure 16 shows the difference between one and four wall layers while Figure 17 shows the difference between four and ten roof/floor layers.

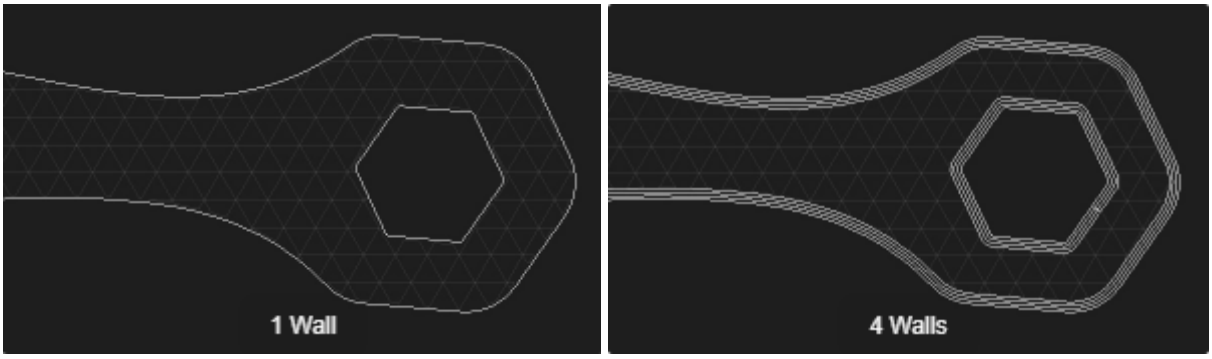

Figure 16. Screen Captures Illustrating Part with 1 Wall Layer on the Right and 4 Wall Layers on the Left ("Eiger," 2016)

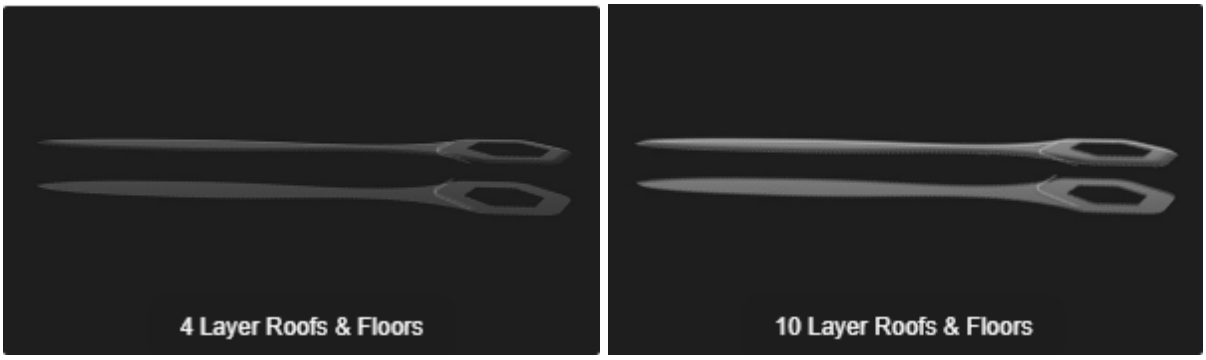

Figure 17. Screen Captures Illustrating Part Roof and Floor Layers 4 Layers on the Right and 10 Layers on the Left ("Eiger," 2016)

The layering can be changed to have fiber and nylon or only nylon depending on the user preference; while having a minimum of one top and one bottom nylon layers. The software also allows the user to enable the use of supports to provide additional stability to the part during manufacturing that can be removed later.

Fiber start location can be changed manually for each layer or the user can choose to use the default setting which changes the start location on each layer to prevent overlapping which creates week spots. Figure 18 shows the fiber (highlighted in blue) start location.

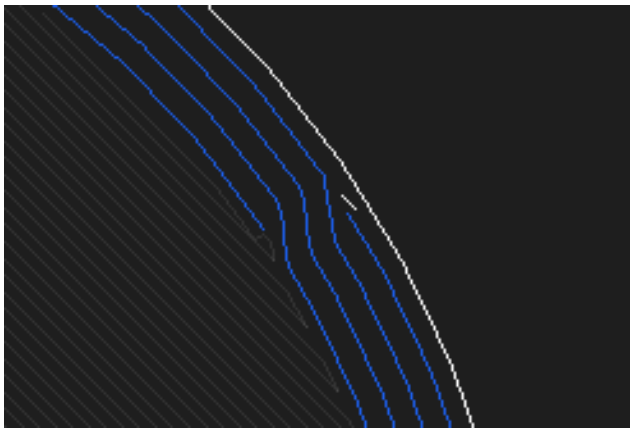

Figure 18. Screen Capture Illustrating Fiber Start Location ("Eiger," 2016)

Supports are columns of nylon that are added to hold up some parts of the structure to maintain structure stability during printing (Figure 19). The supports can be removed after the part is finished. Also, Eiger gives the user the ability to use brim which is an anchor that increases the contact area between the part and the print bed. It is used to add more area of contact between the print bed and the part being manufactured to minimize deformation. Figure 20 represents parts with or without brim.

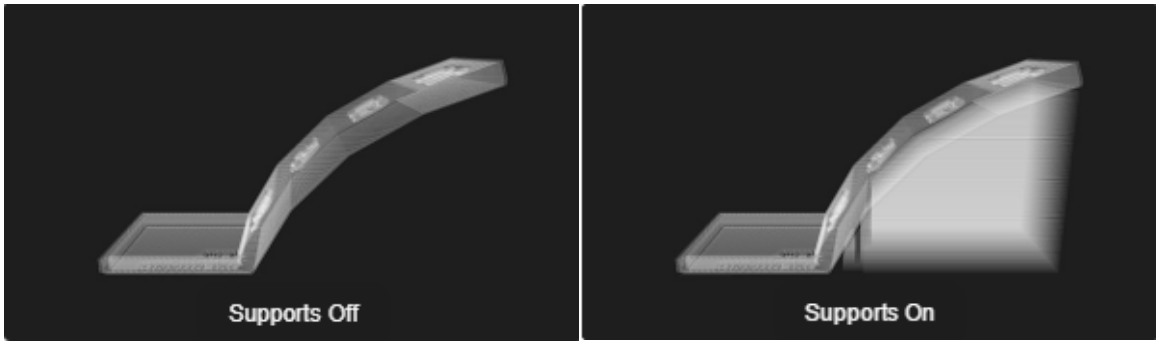

Figure 19. Screen Captures Illustrating Part without Supports on the Right, Part with Supports on the Left ("Eiger," 2016)

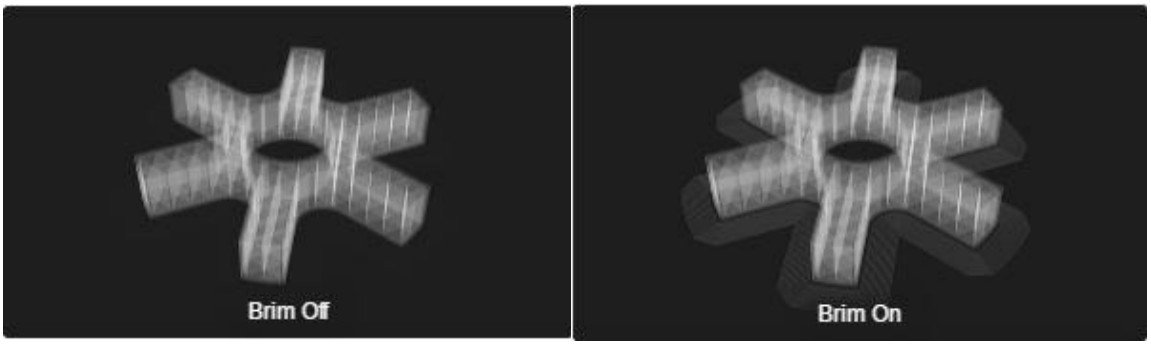

Figure 20. Screen Captures Illustrating Part without Brim on the Right, Part With Brim on the Left ("Eiger," 2016)

III. Methodology

Chapter Overview

This chapter describes the manufacture and testing procedures used in this study. Testing was performed in accordance with ASTM standard D3039 - *Standard Test Method for Tensile Properties of Polymer Matrix Composite Materials* (ASTM Standard D3039/D3039M, 2014). When testing composite specimens with a 0˚ unidirectional fiber orientation, the D3039 standard recommends each test specimen have width, length, and thickness dimensions of 15 mm × 250 mm × 1 mm, respectively. In attempting to build specimens with the recommended dimensions, an issue arose since the minimum layer thickness for the MarkOne® printer is limited to 0.125mm. Thus, using the MarkOne® printer to manufacture specimens with the recommended dimensions would result in test specimens with no more than eight layers. This restriction would clearly constrain the factor-space of this investigation. However, it should be noted that dimensions listed in the D3039 standard are recommendations only and can be varied if the geometry requirements provided by the standard are met. Thus, the specimens used in this study were each manufactured to have 24 layers and width, length, and thickness dimensions of 15 mm × 250 mm × 3 mm, respectively. The dimensions are shown in Appendix A. Finally, this chapter summarizes statistical analysis and the calculations used to obtain the mechanical properties.

Experimental Factors Used in the Study

The purpose of this investigation was to develop a mathematical model describing the functional relationship between the tensile strength of additively manufactured composites and several additive manufacturing build process parameters. For this study, the following four build process parameters were included as factors: (1) the build time between successive layers, (2) the arrangement of the fiber and nylon layers, (3) the fiber start location, and (4) whether or not

supporting material was used during the build process. Each of these factors were tested at two levels (high and low), the level settings used each factor are described in the following paragraphs. For factors (2 – 4) the level setting were explicitly controlled using the Eiger® software, while the build time between successive layers was set by printing 5 specimens at the same time which adds time between quadruples the time between specimen layers compared to printing 1 specimen at a time.

Factor 1: Build time between successive layers

Initially, each factor has two level setting. For time between layers the minimum time corresponded to printing only one part at a time (1PAT); while the maximum time corresponded to printing five specimens at a time (5PAT) with 1PAT being the default. Table 3 shows the detailed approximation of layer print time for each print setting. Due to layers 1 through 5 using brim which adds more time to both manufacturing setting compared to layers 6 through 24. This factor was included to study whether or not the time difference might decrease layer bonding that may result in reducing matrix to fiber load transfer.

Table 3. Detailed Specimen Layer Printing Time

Layer Number	Layer Type	Layer Time per Part (1PAT) Min:Sec	Total Time Between Layers (5PAT) Min:Sec
1 - 5	Nylon	22:27	112:15
1 - 5	Fiber	17:00	85:00
6 - 24	Nylon	9:18	46:30
6 - 24	Fiber	8:06	40:30

Factor 2: Arrangement of Fiber and Nylon layers

Fiber/Nylon layering the two setting are shown in Figure 21 with every layer having a thickness of 0.125mm with setting (A) being the default. In both setups, the total number of fibers where 10 layers out of 24. Eiger's recommends the use of 4 roof and floor layers instead of 1 layer for better surface finish and weathertightness. However, these two properties are not critical to this research and the resulting layering is shown in Figure 21. This factor was included in this research to study whether fiber-to-fiber or fiber-nylon bonding could introduce discontinuity in the load transfer between matrix and fiber.

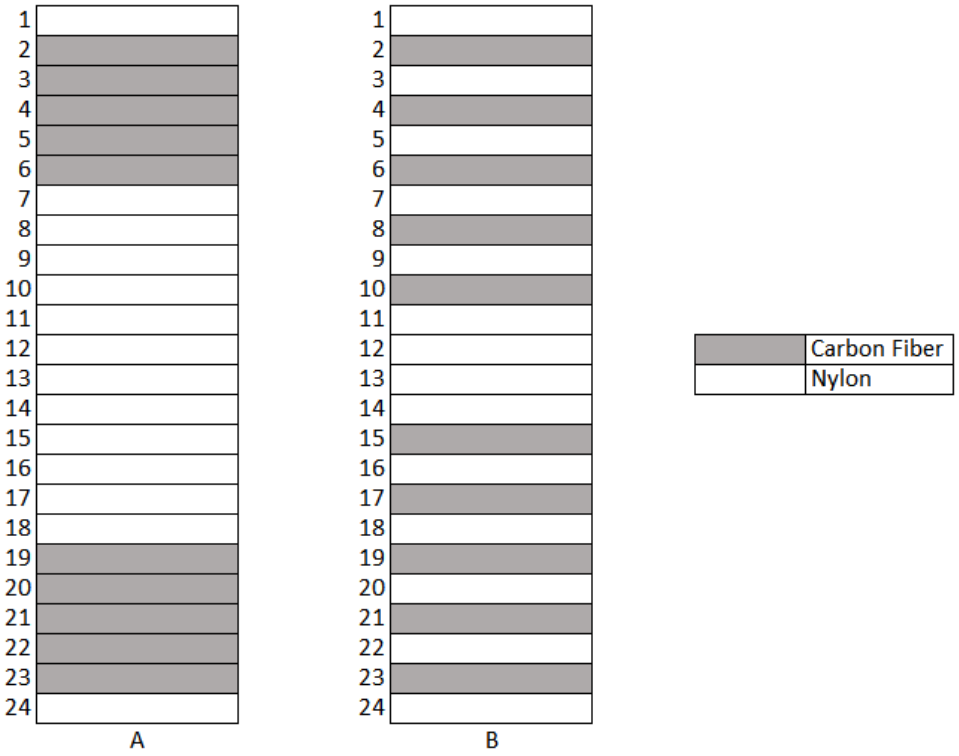

Figure 21. Two Fiber/Nylon Layup Sequence (A) Default, (B) Effect Setting

Factor 3: Fiber start location

Fiber start location setting will be using 0-50% as a start location on the specimens which will start the fiber at the ends of the specimens while alternating between both ends with each fiber layer (Figure 22, Figure 23), and the other setting will be using the default setting provided by Eiger which changes the start location percentage with every layer to insure no start location overlapping at any point that may introduce discontinuity in the specimens (Figure 24); 0-50% will be the default setting. Studying the use of support can be achieved using Eiger option of lifting the specimen of the print bed by 20 layers and using support structure to support the specimens while printing, while the default is not using any supports. This factor was studied to show the potential effect of fiber discontinuity in the concentric rings printing method.

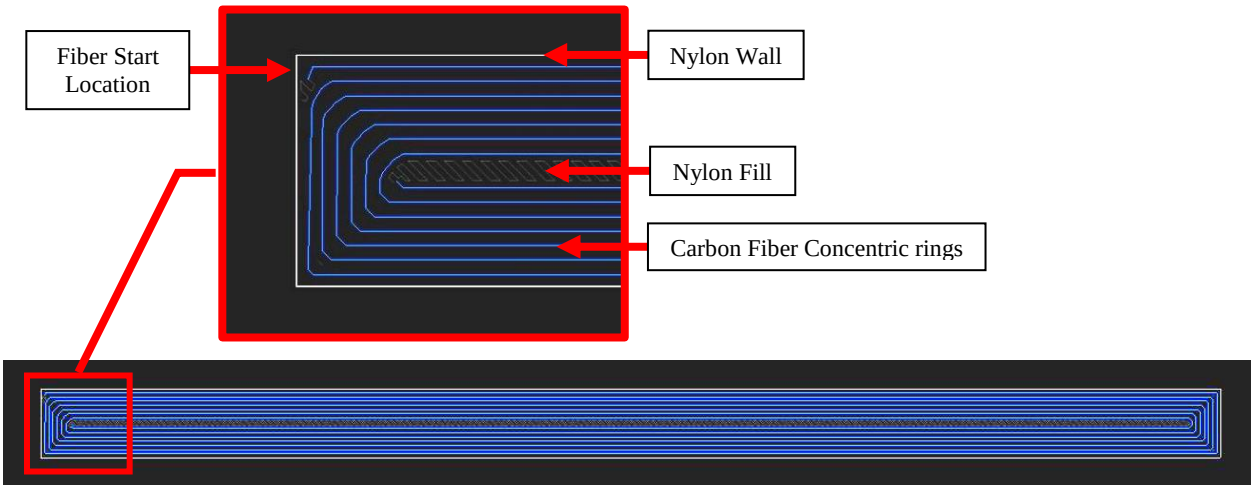

Figure 22. Screen Capture Illustrating Specimen 0% Fiber Start Location ("Eiger," 2016)

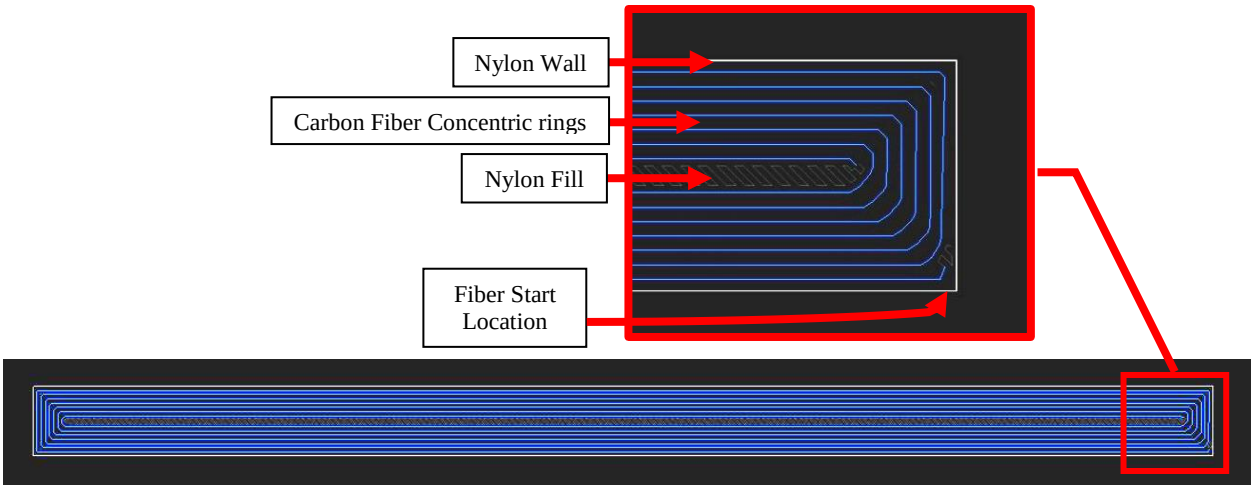

Figure 23. Screen Capture Illustrating Specimen 50% Fiber Start Location ("Eiger," 2016)

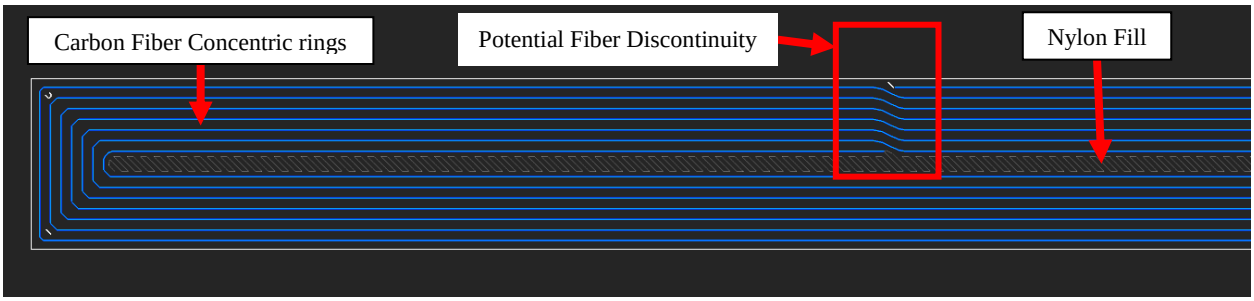

Figure 24. Screen Capture Illustrating Specimen One of the Possible Fiber Start Locations Egier's Default Setting ("Eiger," 2016)

Factor 4: Use of supporting material

Support material will be used in two settings; the default shown in Figure 25 where the specimen will be manufactured on the print bed without using supports and the other setting shown in Figure 26 will be manufactured using Eiger's support setting which adds a removable 20 layer support before printing the specimen. In this case the software builds the supports parallel to the specimen length and the print bed. This factor was included to study whether or not the use of supports weakens the structure into which the specimen will be printing that might affect the specimens' strength.

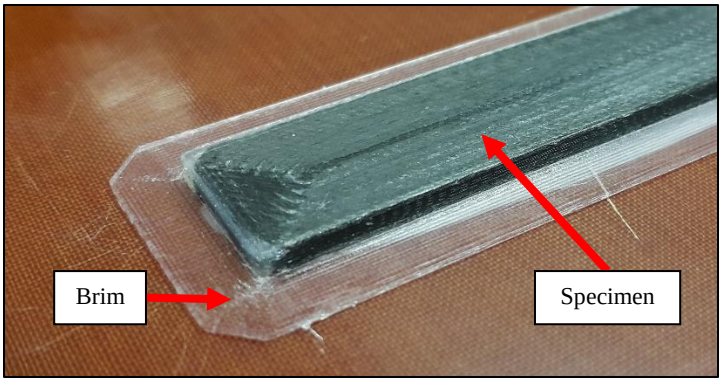

Figure 25. Specimen Manufacured Without the Use of Support Material

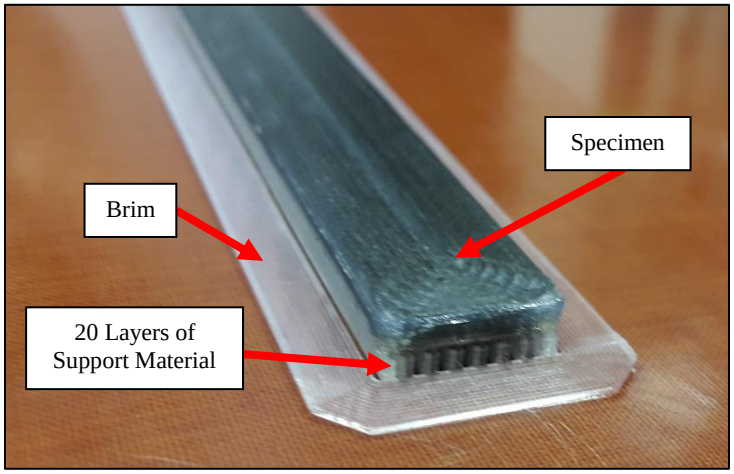

Figure 26. Specimen Manufactured Using Support Material

Selecting Test Points

For the selected factors and factor level settings described above, a full-factorial design (2^4) would require testing specimens at 16 design points. The data produced from such a test would provide information on the effect that each factor has on the tensile strength of the specimens. A full-factorial design would also provide information of the effect that the 2-, 3-, and 4- level interaction has on the tensile strength. However, performing this test with five replicates at each design point, as required by ASTM D3039, would require eighty specimens to be manufactured and tested. Due to time and cost limitations, a 2^{4-2} fractional factorial design

was chosen to gain information on the main effects. This studies the one level interaction (Four test points) and compare it to the fifth default test point that will be considered a baseline. Table 4 Shows the full-factorial design and the selected test points.

Table 4. Test points for the 2^4 Full Factorial Design (rows corresponding to the fraction of test points used in the current study have been shaded)

Test Point Number	Build time between successive layers	Arrangement of Fiber and Nylon layers	Fiber start location	Support
1	-	-	-	-
2	+	-	-	-
3	-	+	-	-
4	+	+	-	-
5	-	-	+	-
6	+	-	+	-
7	-	+	+	-
8	+	+	+	-
9	-	-	-	+
10	+	-	-	+
11	-	+	-	+
12	+	+	-	+
13	-	-	+	+
14	+	-	+	+
15	-	+	+	+
16	+	+	+	+

-	Default Setting
+	Effect setting
	Selected test points

Table 5. Test Points Used in the Current Study

Test Point Number	Build time between successive layers	Arrangement of Fiber and Nylon layers	Fiber start location	Support
1	-	-	-	-
2	+	-	-	-
3	-	+	-	-
4	-	-	+	-
5	-	-	-	+

- Default Setting
+ Effect setting

Manufacturing Specimens

Five specimens are required for each test point in accordance to ASTM D3039. The 25 specimens were manufactured while recording manufacturing time/date, the changes in material lot, print bed leveling, and specimen weight to minimize unexplained variance. The manufacturing data is presented in Appendix B. The manufacturing of the 25 specimens required four fiber lots, and the print bed was leveled five times.

After manufacturing the specimens, the width and thickness of each specimen was recorded and by averaging the gage measurements many specimens were not meeting the ASTM D3039 standard tolerance limitations when compared to the designed 3mm and 15 mm. However, most of the specimens met the tolerances ±1% of width and ±4% of thickness when compared to the mean of specimen's dimensions. There was only one specimen that exceeded the ±1% width tolerance, however this specimen was used due to the difficulty of reproducing and controlling the tolerances and due to the specimen exceeding the tolerances by less than -0.05% of width; this specimen was used in this research. specimen measurements are presented in Appendix B.

Eiger recommends using 2 wall layers for better surface finish and weather-tightness. The use of triangle fill is also recommended for optimal dimensional accuracy, print time, and strength to weight ratio. 50% fill density is recommended to decrease printing time. However, all specimens used 1 wall layer, 7 fiber concentric rings, and rectangular fill with 100% fill density.

During manufacturing of specimens with the default setting of fiber start location (0%-50%) we found that the printer does not start printing exactly at the specified location in Eiger as shown in Figure 22. The fiber filament starts and ends approximately 40mm and ends 23mm respectively from the specimen edge; Figure 27 shows the start location on a 1 layer fiber sample. However, due to the difficulty of correcting this error; because fiber start location is never consistent and this occurs on the user-set as well as the software-set start location this start location will still be considered the 0%-50% start location. This delay of fiber deployment might be because of the distance the fiber must travel from the fiber cutter to the fiber print head which is 610mm (Figure 29).

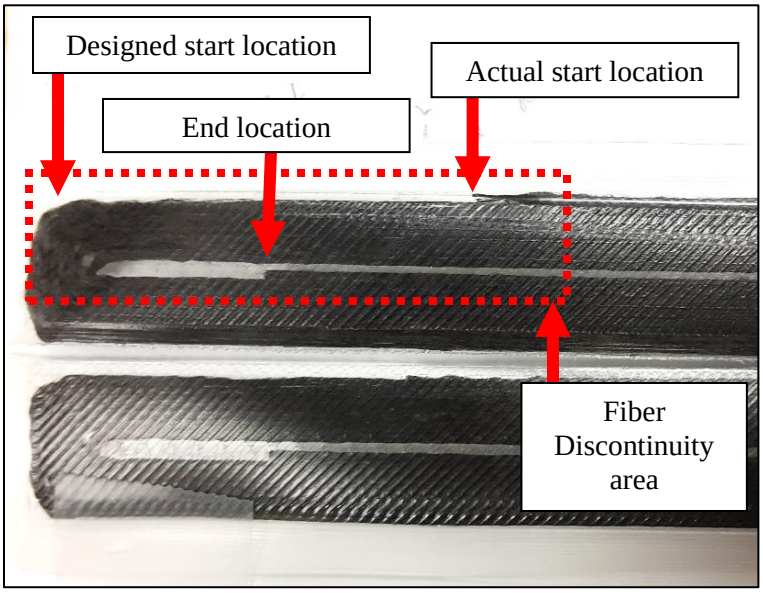

Figure 27. Actual Fiber Filament Start and End Location for 0% and 50% Fiber Start Setting

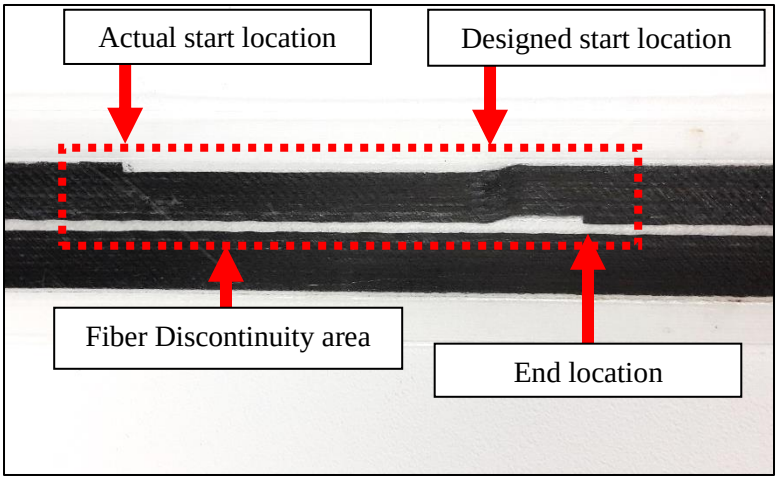

Figure 28. Actual Fiber Filament Start and End Location for Default Start Setting

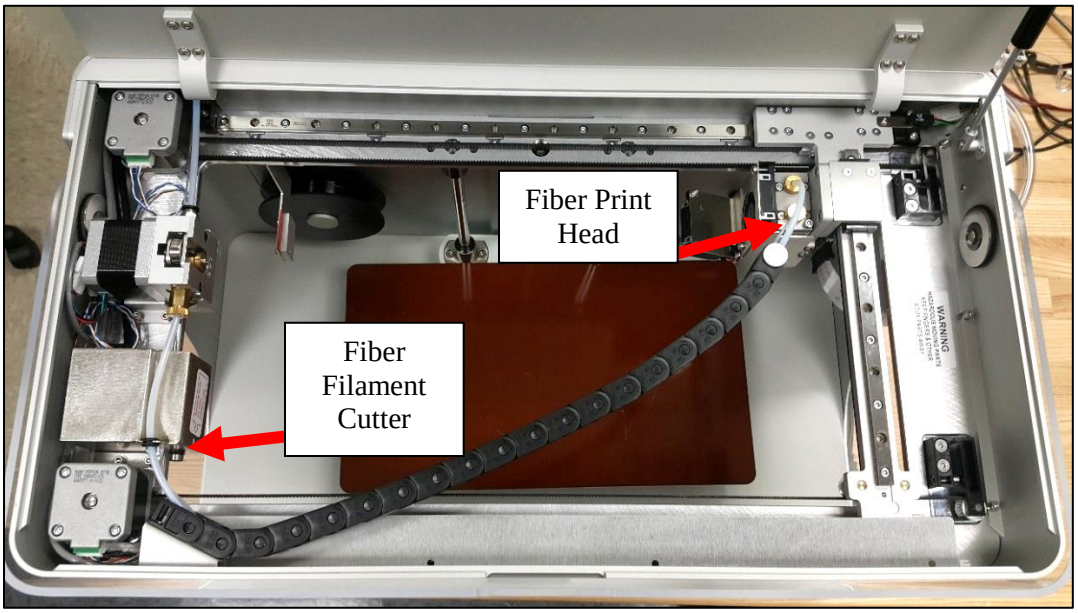

Figure 29. MarkOne 3D Printer Fiber Filament Cutter and Fiber Print Head (Top View)

After manufacturing each specimen, the part was kept on the print bed for at least an hour to cool-down and cure to minimize deformation during storage. All specimens where stored in a dry box until the time of preparing the specimens prior to testing to minimize specimens' moisture absorption; due to the long period between the first manufactured specimen in July 2016 and the time of testing in June 2017.

Tensile Testing

Prior to testing, the order in which the 25-specimen were tested was randomized. The fiberglass tabs dimensions were 100mm × 15mm × 1.5mm with a tensile strength of 68.5 MPa and bonded to the specimens using M-Bond 200 adhesive (Figure 30). Due to the longer tabs used, results from test point 4 could potentially be of lower significance due to both the default and effect setting fiber start locations starting in the tabbed area. Tensile testing was conducted on MTS 810 Material Testing System with test speed at fixed rate of 100N/Sec. Grip pressure was set to 4.82633N/mm^2 (700 psi), room temperature was 24˚C and 71% relative humidity. A MTS 632.13E-20 extensometer was used and placed in the middle of the gage length. Figure 31 shows specimen setup on the machine with the extensometer installed, while Figure 32 shows specimen setup from the side before installing extensometer. Tabs, grip pressure, and test speed calibrated using 8 similar samples that resulted in the most consistence failure results. Tensile Test calibration specimens' results are included in Appendix C. The data obtained from the tensile test were the applied force (N), displacement (mm), strain (mm/mm), and the time of recording at a rate of 10 data recordings per second. Tensile test failure code was then recorded for each specimen per D3039 (ASTM Standard D3039/D3039M, 2014).

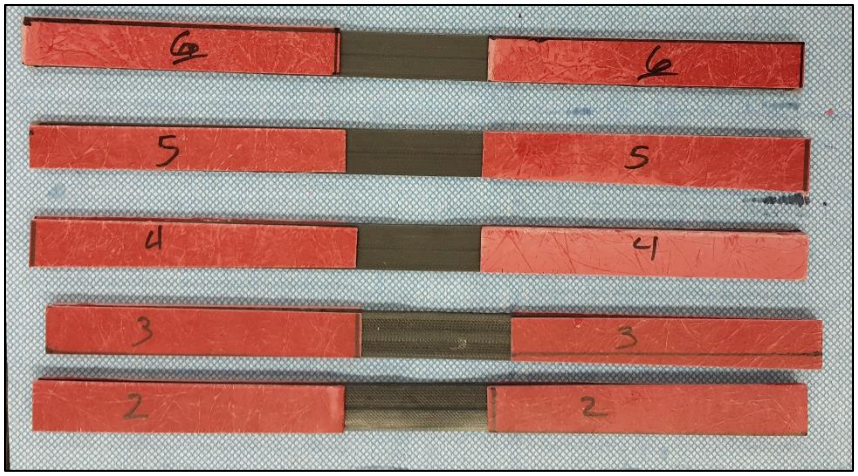

Figure 30. Specimens After Installing Tabs

Figure 31. Specimen Setup on MTS 810 with extensometer installed

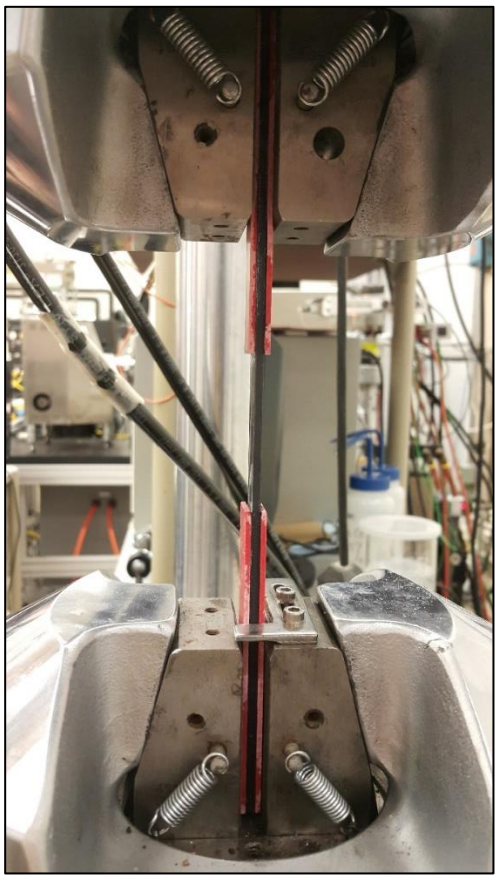

Figure 32. Specimen Setup from the Side, without Extensometer Installed

Statistical Analysis

Following the tensile test, a liner regression analysis was performed to estimate the statistical relationship between the dependent variable and the explanatory variables. This relationship is expressed as a linear model of the form shown in Eq. 1

$$y_i = \beta_o + \beta_1 x_{i1} + \beta_2 x_{i2} + \ldots + \beta_n x_{in} + \varepsilon_i \quad (1)$$

where y_i denotes the observed response for specimen $i = 1,2,\ldots,N$, x_{ij} is the value of explanatory variable $j = 1,2,\ldots,n$ for specimen i, β_j is the estimated regression coefficient for explanatory variable j, and ε_i is the error between the linear model and the observed response for specimen i.

IV. Analysis and Results

Chapter Overview

This chapter will present the results of the tensile test and statistical analysis. First, the stress-strain curves for the 25 specimens were plotted. Next, the ultimate tensile strength, ultimate tensile strain, and failure modes were presented. Finally, a regression analysis was performed and the model results and validation was presented.

Mechanical Properties

The objective of this study was to develop a statistical model describing the functional relationship between several additive manufacturing build process factors and the ultimate tensile strength of CFRP specimens. This chapter details the methods used to analyze the test data and produce an estimate of this relationship. First, the raw test results are presented graphically to highlight any inconsistencies that were observed in failure process. Next, the data are analyzed using linear regression to produce the estimate of the relationship.

From the data obtained during testing, the tensile stress experienced by each specimen was calculated at each observation point as

$$\sigma_{ij} = \frac{P_i}{A_j}. \tag{2}$$

where A_j is the average specimen cross-sectional area (mm^2) for specimen j, P_i is the tensile force recorded at observation point i, and σ_{ij} is the computed tensile stress (MPa) for specimen j at observation point i. Additionally, the strain level, ε_{ij}, was recorded at each observation point for every specimen. Figure 33 through Figure 37 show the stress-strain relationship for all samples within each test point. These figures can be used to reveal significant differences in the failure process for each specimen within a test point. The figures show little

variation in the failure process and the ultimate tensile strength observed at each test. One notable exception is specimen number 18, (Figure 35) showed significantly lower ultimate tensile stress compared to the rest of the samples tested at this test point.

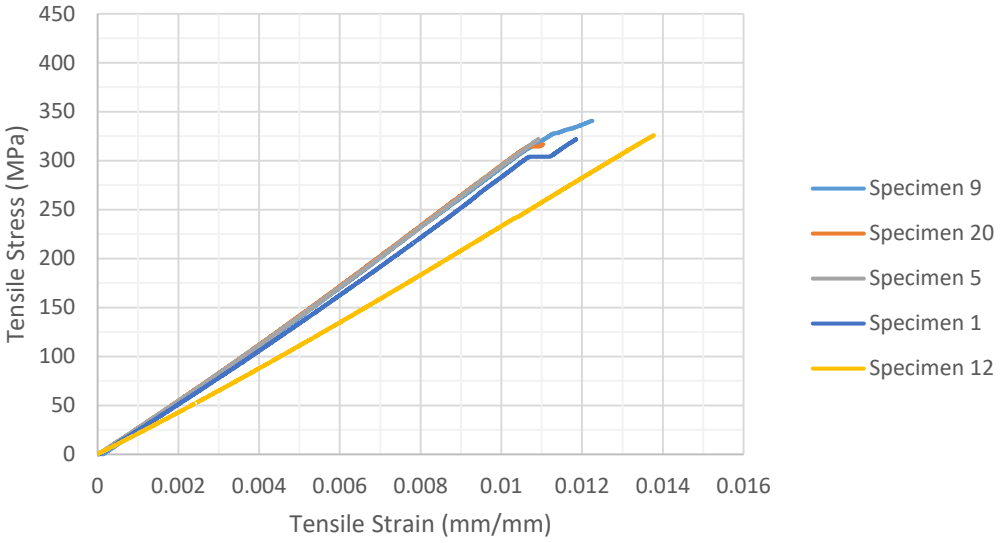

Figure 33. Tensile Stress vs Strain relationship for Specimen in Test Point 1

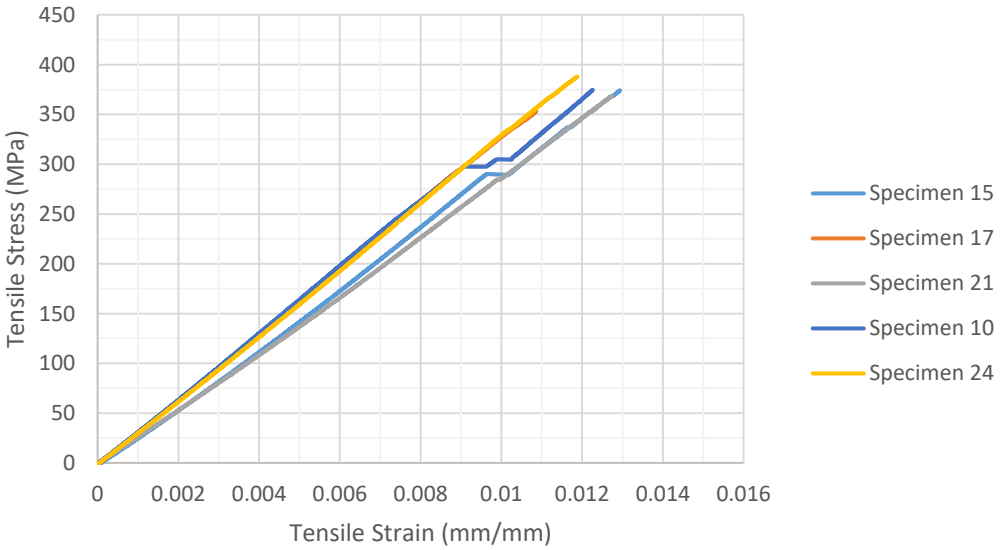

Figure 34. Tensile Stress vs Strain relationship for Specimen in Test Point 2

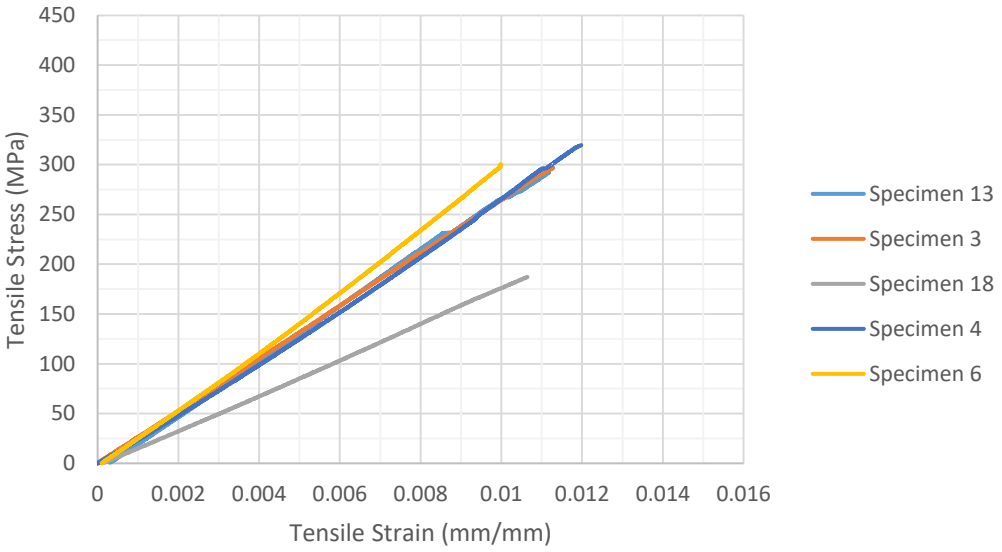

Figure 35. Tensile Stress vs Strain relationship for Specimen in Test Point 3

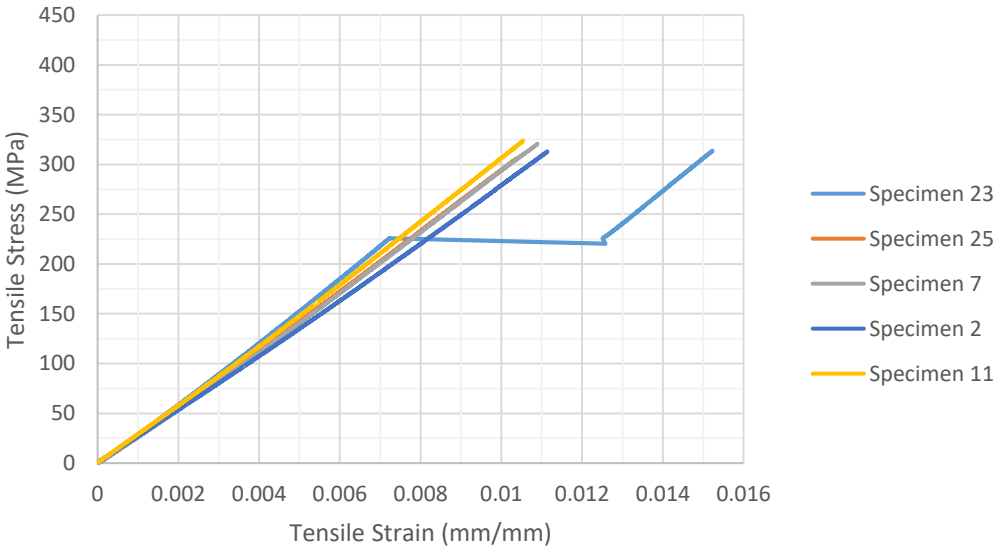

Figure 36. Tensile Stress vs Strain relationship for Specimen in Test Point 4

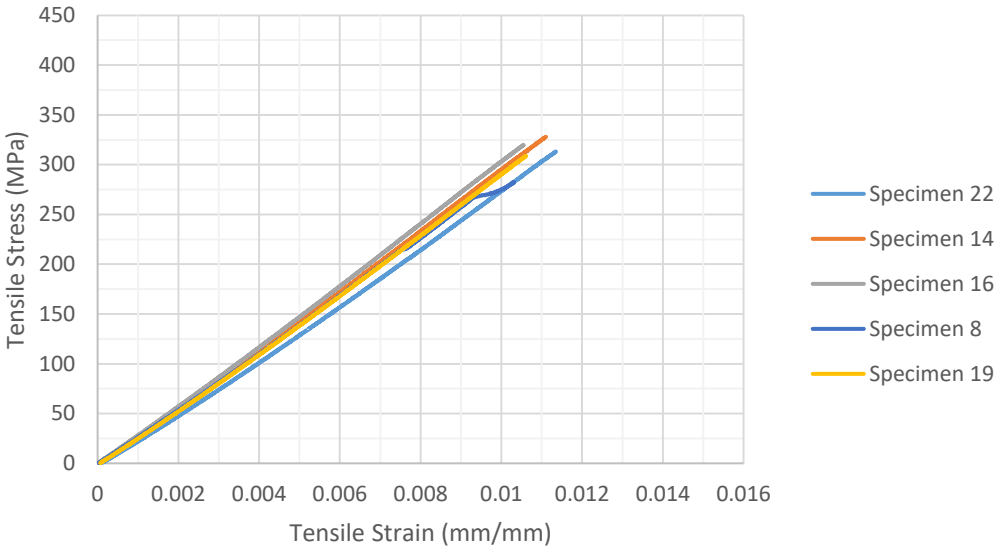

Figure 37. Tensile Stress vs Strain relationship for Specimen in Test Point 5

Test Results and Failure Modes

For specimen $j = 1, \ldots, 25$, the ultimate tensile strength UTS_j was computed as

$$UTS_j = \frac{\max_i [P_{ij}]}{A_j} \tag{3}$$

Where A_j is the average cross-sectional area for specimen j, $\max_i [P_{ij}]$ is the maximum tensile load P_i observed for specimen j.

The modulus of elasticity (GPa) was computed as the slope of the stress-strain curve

$$E = \frac{\Delta\sigma}{\Delta\varepsilon} \tag{4}$$

Where $\Delta\sigma$ is the difference in applied tensile stress between the two strain points (Mpa) and $\Delta\varepsilon$ is the difference between the two strain points. The failure data obtained from testing the 25 specimens are shown in Table 6. The table includes the calculated ultimate tensile strength for each specimen, the recorded ultimate tensile strain, maximum recorded displacement, and

specimen failure mode per Figure 38. Failure mode were difficult to determine due to the longer tab used in this test; for example, specimens 12, 17, 21, and 25 failed at the grip with fracture to both specimens and tabs. Representative pictures of specimens after testing are included in Appendix D.

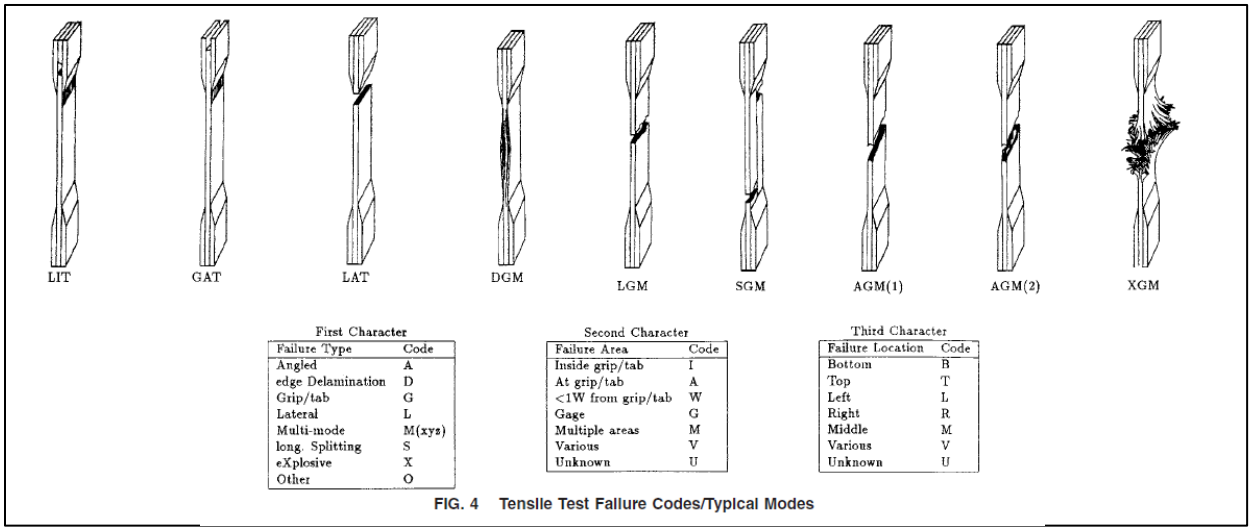

First Character

Failure Type	Code
Angled	A
edge Delamination	D
Grip/tab	G
Lateral	L
Multi-mode	M(xyz)
long. Splitting	S
eXplosive	X
Other	O

Second Character

Failure Area	Code
Inside grip/tab	I
At grip/tab	A
<1W from grip/tab	W
Gage	G
Multiple areas	M
Various	V
Unknown	U

Third Character

Failure Location	Code
Bottom	B
Top	T
Left	L
Right	R
Middle	M
Various	V
Unknown	U

FIG. 4 Tensile Test Failure Codes/Typical Modes

Figure 38. Tensile Tesnt Failure Codes/Typical Modes (ASTM Standard D3039/D3039M, 2014)

Table 6. Specimen Ultimate Tensile Strength, Ultimate Tesnile Strain, Maximum Displacement, and Recorded Failure Mode

Observation Number	Specimen Number	Test Point	Ultimate Tensile Strength (MPa)	Ultimate Tensile Strain (mm/mm)	Modulus of Elasticity (GPa)	Maximum Displacement (mm)	Failure Mode
1	9	1	340.48	0.01225	29.896	2.22	LGM
2	20	1	316.84	0.01103	29.801	2.20	LIB
3	5	1	322.05	0.01092	29.695	2.19	LWB
4	1	1	321.77	0.01185	28.508	2.16	LIT
5	12	1	325.99	0.01377	23.862	2.26	OIB
6	15	2	374.08	0.01293	30.110	2.60	LAB
7	17	2	353.18	0.01086	33.254	2.39	OIB
8	21	2	368.40	0.01273	28.976	2.51	OVT
9	10	2	374.68	0.01226	32.427	2.57	LIB
10	24	2	387.96	0.01188	33.153	2.61	LIB
11	13	3	292.97	0.01117	27.314	2.04	LIT
12	3	3	296.90	0.01127	26.474	2.15	LGM
13	18	3	187.19	0.01064	17.950	1.87	LIB
14	4	3	319.65	0.01197	27.070	2.13	LAT
15	6	3	300.39	0.00999	30.259	1.92	LWM
16	23	4	313.67	0.01522	17.590	2.18	LIB
17	25	4	305.87	0.01037	29.631	2.07	OIB
18	7	4	320.62	0.01088	29.773	2.19	LAT
19	2	4	312.96	0.01113	28.043	2.07	LAB
20	11	4	323.77	0.01053	30.791	2.18	LIT
21	22	5	313.05	0.01135	28.025	2.29	LIT
22	14	5	328.06	0.01110	29.864	2.48	OIB
23	16	5	319.81	0.01054	30.537	2.37	LIB
24	8	5	282.52	0.01031	28.589	2.07	LIT
25	19	5	308.76	0.01061	29.498	2.08	LWM

Figure 39 shows a scatter plot of the ultimate tensile stress versus the ultimate tensile strain plotted for each specimen and grouped by test point. The results clearly show that higher ultimate tensile strengths are obtained at test point 2 compared to the other test points.

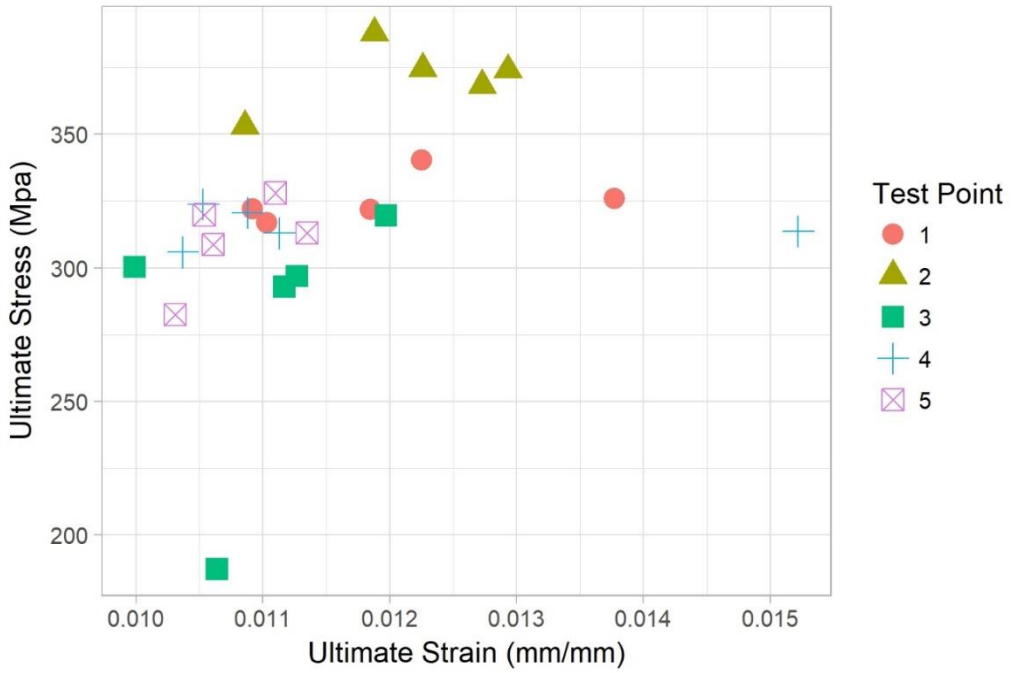

Figure 39. Scattered Plot of Ultimate Tensile Stress versus Ultimate Tensile Strain for Each Specimen

Figure 40 is a scatterplot showing the observed ultimate tensile strengths versus the corresponding ultimate tensile strain grouped per the observed failure mode. This figure shows no pattern regarding failure mode and ultimate tensile stress. Figure 41 shows the calculated modulus of elasticity with the mean and standard error for each test point. This figure shows higher modules of elasticity for test point 2 compared to the other test points.

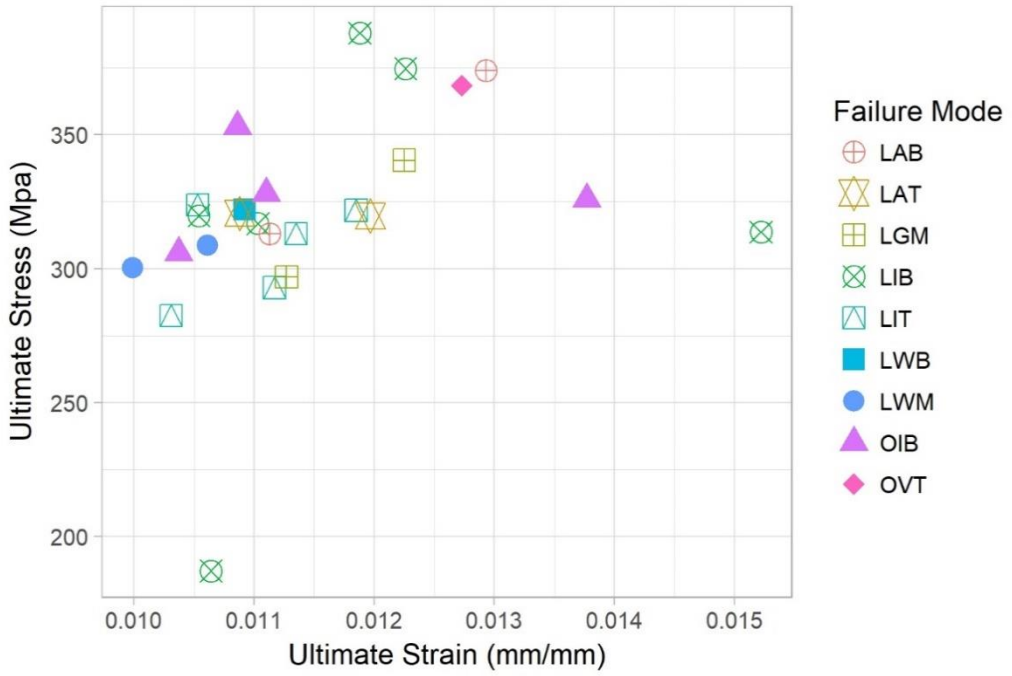

Figure 40. Scattered Plot of Ultimate Tensile Stress versus Ultimate Tensile Strain for Each Failure Mode

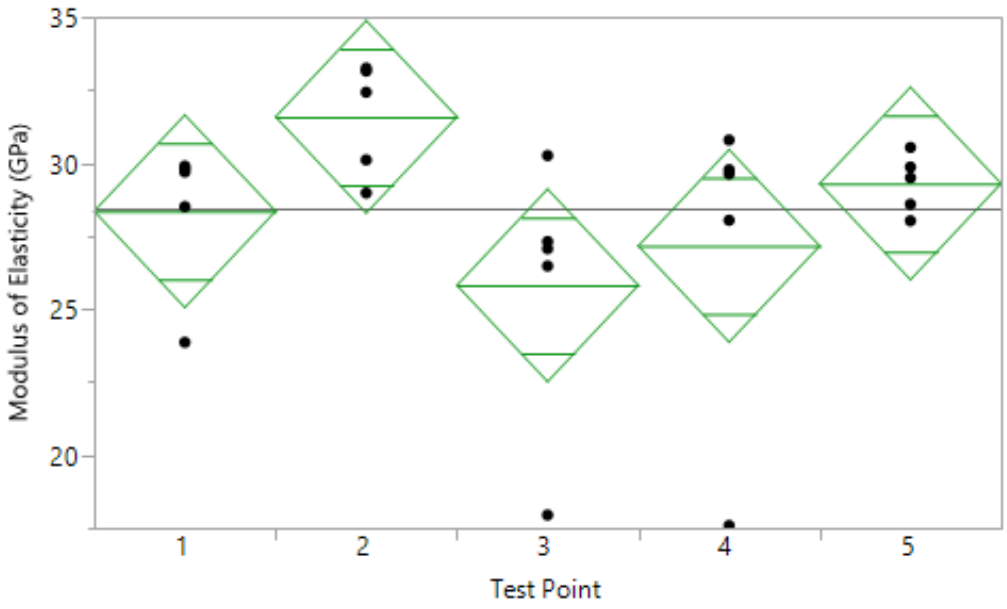

Figure 41. Scattered Plot of Modulus of Elasticity Grouped by Test Point

Statistical Analysis

Regression analysis was performed once using the 25 specimens and once without specimen 18 due to the lower ultimate tensile strength for this specimen. The dependent variable was the ultimate tensile strength and the explanatory variables were the four factors with 0 being the low (default) setting and 1 as the high setting. Table 7 shows the estimated regression coefficients β, error variance ε, t stat, P-value, and the upper and lower 95% confidence intervals. The regression model result is presented in Eq. 5.

Table 7. Regression Results for All 25 Specimens

	Coefficients β	Standard Error ε	t Stat	P-value	Lower 95%	Upper 95%
Intercept	325.430	11.574	28.116	1.491E-17	301.286	349.574
Build time between successive layers (X_1)	46.237	16.369	2.825	0.010468	12.093	80.382
Arrangement of fiber and nylon layers (X_2)	-46.006	16.369	-2.811	0.010801	-80.150	-11.861
Fiber Start location (X_3)	-10.045	16.369	-0.614	0.546370	-44.189	24.100
Use of supporting material (X_4)	-14.986	16.369	-0.916	0.370824	-49.131	19.159

$$UTS_i = 325.4 + 46.2(X_1) - 46.0(X_2) - 10.04(X_3) - 14.98(X_4) + \epsilon_i \quad (5)$$

Figure 42 shows a Quantile-Quantile plot (QQ plot) for all 25 specimens with a 95% confidence band as the dashed lines; some of the data points in this fit are outside the confidence interval area. Figure 43 is a Bubble Plot of Cook's Ds studentized residuals, and Hat-Values for All 25 Specimens, with the size of the circle representing the influence of the data point on the whole dataset. Figure 44 shows Cook's distance plot, which also estimates the influence of a data point on a regression analysis; a higher Cook's distance represents a stronger the impact.

Specimen 18 (observation 13) has the highest effect on the dataset which is represented in Figure 43 as the green circle and in Figure 44 as observation 13. Figure 45 shows the residual versus fitted values variance plot. Due to the negative slope relationship, the assumption of constant variance is not valid; this regression model does not pass validation and the regression will be performed after the removal of specimen 18.

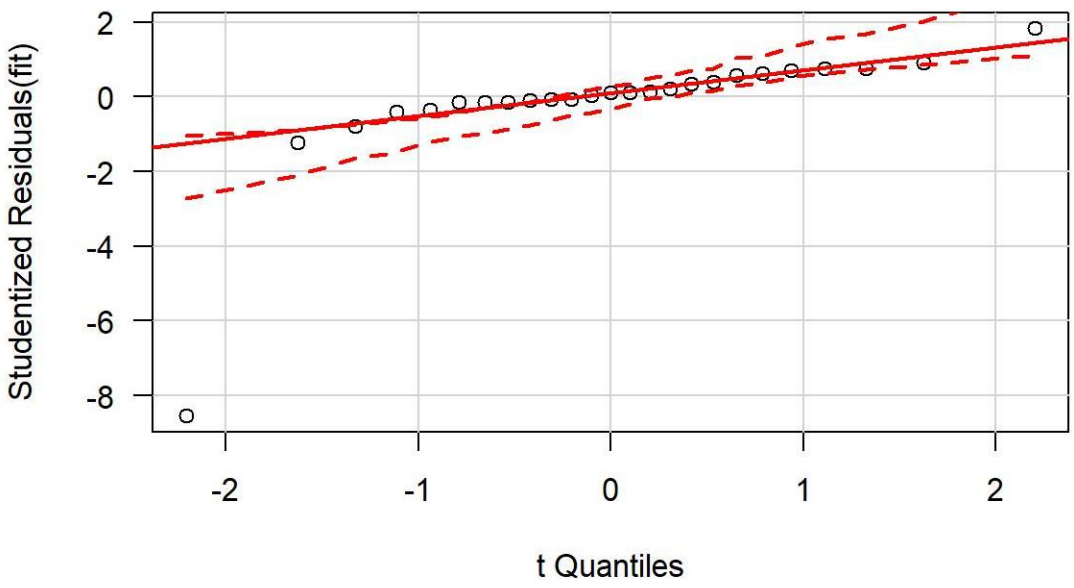

Figure 42. QQPlot for All 25 Specimens

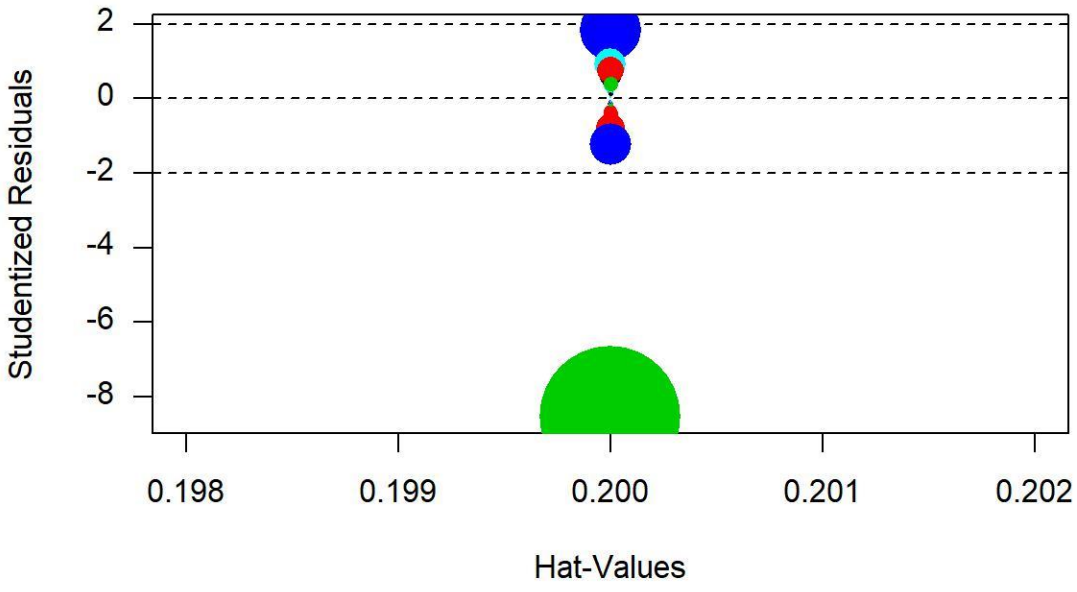

Figure 43. Bubble Plot of Cook's Ds Studentized Residuals, and Hat-Values for All 25 Specimens

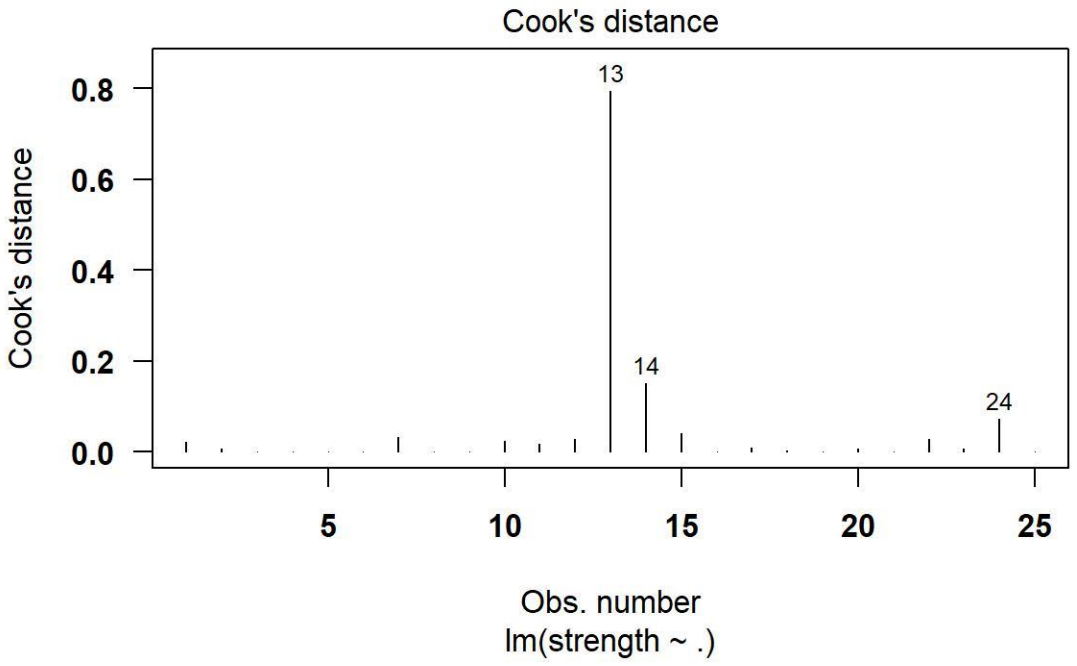

Figure 44. Cook's Distance Plot for All 25 Specimens

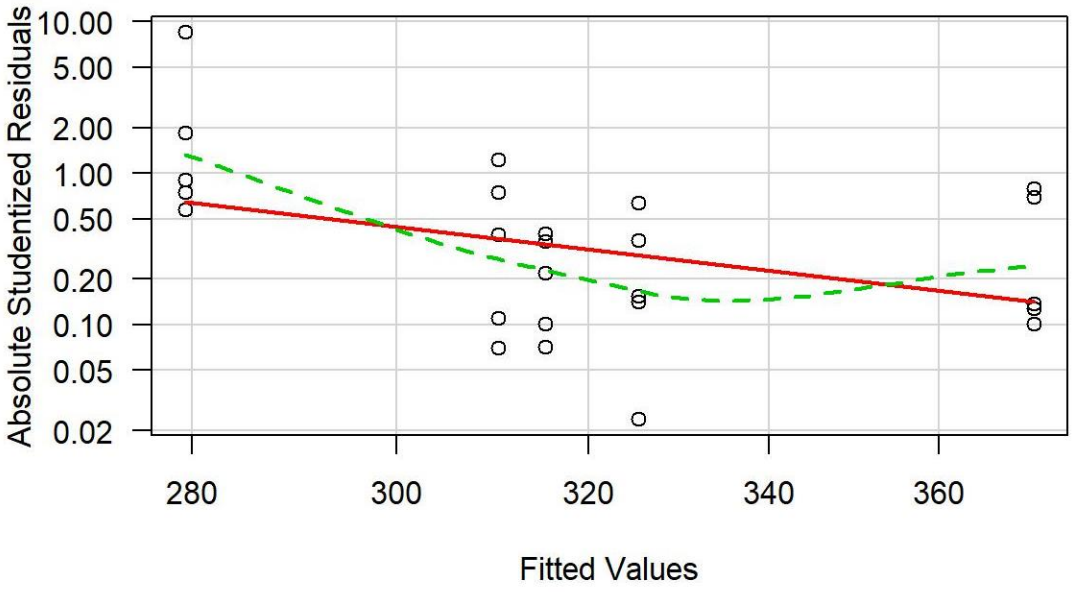

Figure 45. Variance Plot for All 25 Specimens

Table 8 shows the estimated regression coefficients β, error variance ε, t stat, P-value, and the upper and lower 95% confidence intervals for the regression model after deleting specimen 18. The build time between successive layers (Test Point 2) effect has a positive effect on the ultimate tensile strength. This might be a result of the increased temperature stability and warmer temperatures inside the printing area the longer the print time; which could help in slowing the rate of cooling and material curing, thus decreasing deformation of the individual layers and the specimen. The rest of the factors have a negative effect on the ultimate tensile strength with only arrangement of fiber and nylon layers (Test Point 3) having P-value lower than α of 0.05. The negative effect of the fiber arrangement could have mean a result of the better bonding between the layers of fiber compared to the bonding between the layers of nylon and fiber. This could have resulted in better load transfer which higher fiber layers to contribute in resisting the applied tensile load. However, due to the longer tabs used in this tensile test the

effect of fiber start location (Test Point 4) could have potentially been minimized because fiber start location in both the default and effect setting were inside the tabbed area with the effect setting fiber start location being closer to the tab ends. The non-significant effect of the supporting material shows that in cases where the supporting structure is manufactured parallel to the fiber direction supporting material does not highly effect the final part tensile strength. The regression model result is presented in Eq. 6.

Table 8. Regression Results Without Specimen 18

	Coefficients β	Standard Error ε	t Stat	P-value	Lower 95%	Upper 95%
Intercept	325.430	5.393	60.337	3.576E-23	314.141	336.719
Build time between successive layers (X_1)	46.237	7.628	6.062	7.876E-06	30.273	62.202
Arrangement of fiber and nylon layers (X_2)	-22.948	8.090	-2.836	0.010550	-39.881	-6.015
Fiber Start location (X_3)	-10.045	7.628	-1.317	0.203544	-26.009	5.920
Use of supporting material (X_4)	-14.986	7.628	-1.965	0.064242	-30.951	0.979

$$UTS_i = 325.4 + 46.2(X_1) - 10.045(X_2) - 10.04(X_3) - 14.98(X_4) + \epsilon_i \quad (6)$$

Figure 46 shows a QQ plot after removing specimen 18 with a 95% confidence band as the dashed lines. The apparent deviation from normality is consistent with sampling variability. Figure 47 shows the residual versus fitted values variance plot. Due to the points being within the 95% confidence interval and the horizontal variance relationship this model passes validation.

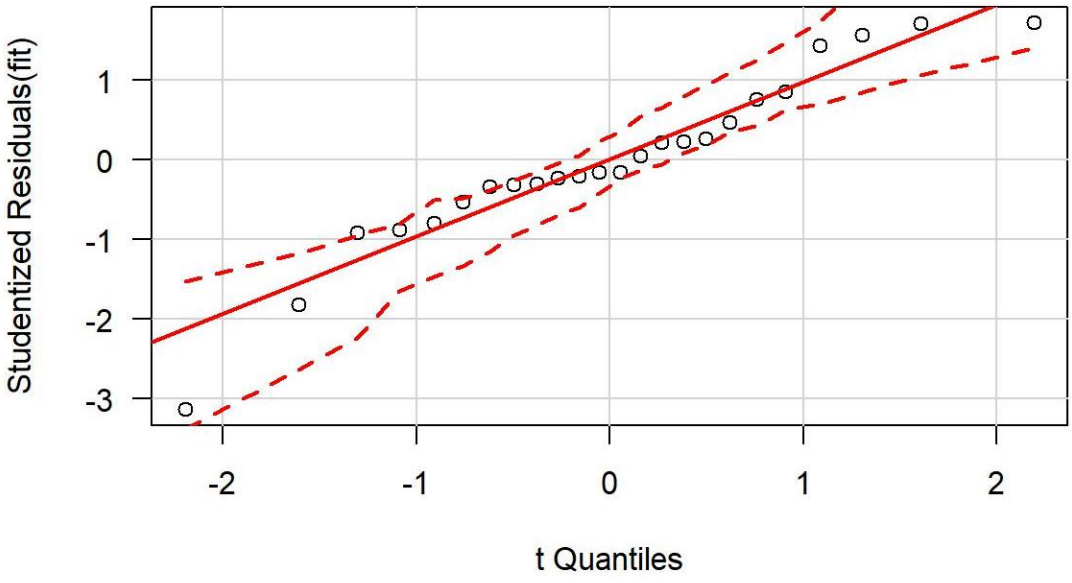

Figure 46. QQPlot Without Specimen 18

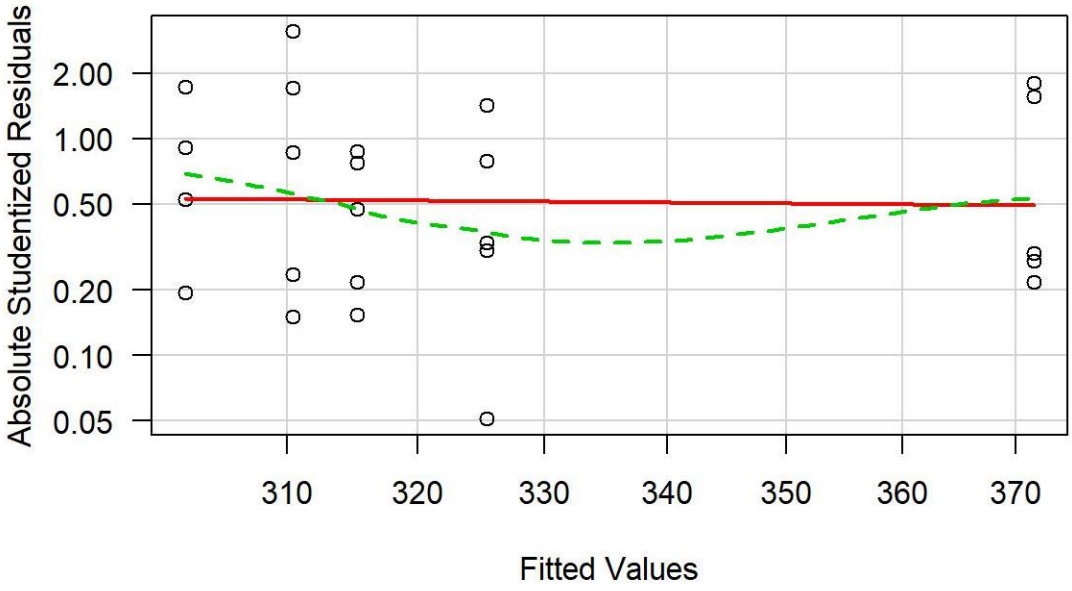

Figure 47. Variance Plot Without Specimen 18

V. Discussion and Conclusion

Chapter Overview

This chapter will discuss the results introduced in the previous chapter. Next, possible future research will be discussed along with recommendation for future research.

Conclusion

In this study, CRP specimens were prepared using a combination of the two additive manufacturing processes; Fuse Filament Fabrication (FFF) and Continuous Filament Fabrication (CFF) from the MarkOne 3D printer. A design of experiment (DOE) was performed between the four factors to obtain information about the impact of the main level interaction. The mechanical properties measured from the five test points were ultimate tensile strength, ultimate tensile strain, and displacement. Specimen 18, one of the five specimens in test point 3 was found to be an outlier. A regression analysis failed validation when performed using the entire dataset. The outlier was removed and the regression model we preformed and validated to identify how each factor effect the ultimate tensile strength. The results showed that the effect setting in the factored had a negative effect on the ultimate tensile strength except the built time between successive layers which showed a significant improvement over the default test point. The fiber start location and the use of supports showed negative non-significant impact. However, the impact on fiber start location could have been minimized due to the longer tabs used in this study. The use of supports shows that the built supporting structure achieves the function of supporting the part without highly impacting the structure overall tensile strength.

This research is only a part of the entire picture of the factors effect on the tensile strength. However, the results show that the higher the parts and printing time the higher the tensile strength; this should be considered when manufacturing parts using the MarkOne 3D

printer. Moreover, the use of the fiber/nylon layer alternating arrangement should be avoided and the use of Eiger's default fiber-sandwich arrangement is recommended unless achieving other mechanical characteristics is desired. When designing more complex parts that require overhanging structures to be built using the MarkOne 3D printer, the overhanging structures should have minimal tensile strength deference's compared to structures from other similar parts. Considering the limitation of the results mentioned above the recommendation of choosing either Eiger deigned fiber start location or controlling each layer's fiber start location cannot be provided. However, considering the weak points in each part like holes, corners, or high load areas and trying to manually check that the software start location does not increase the point's vulnerability.

Future Research

Possible future research could expand on the five test points to cover the two, three, and four level interactions between the four factors included in this research. Table 9 shows the remaining test points. Exploring the possibility of fixing the temperature of the manufacturing area could eliminate the effect of the higher temperatures the longer the manufacturing time which would minimize the temperature effect while studying the build time between successive layers. However, if controlling the manufacturing area temperature is not possible; studying the two-level interactions between the factors and the build time between successive layers while measuring the temperature during manufacturing; could potentially shed light on the importance of controlling the manufacturing environmental conditions.

Expanding testing beyond tensile testing and preforming compression, shear, bending, and torsion to reach better understanding of AM CFRP mechanical properties.

Table 9. Future Research Possible Test Points

Test Point Number	Build time between successive layers	Arrangement of Fiber and Nylon layers	Fiber start location	Support
1	-	-	-	-
2	+	-	-	-
3	-	+	-	-
4	+	+	-	-
5	-	-	+	-
6	+	-	+	-
7	-	+	+	-
8	+	+	+	-
9	-	-	-	+
10	+	-	-	+
11	-	+	-	+
12	+	+	-	+
13	-	-	+	+
14	+	-	+	+
15	-	+	+	+
16	+	+	+	+

-	Default Factor Setting
+	Effect setting
	Future test points

During the test calibration, exploring the possibility of using angled tabs may provide more consistency in failure modes and may show different results in the fiber start location effect test points.

Appendix A. Specimen Dimensions

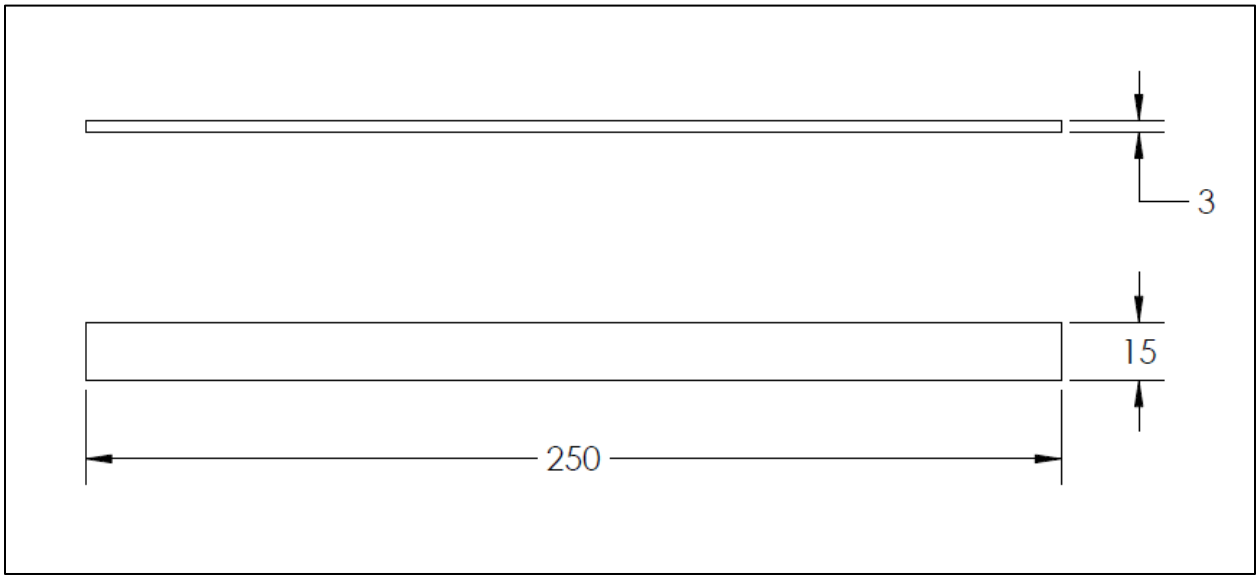

Figure 48. Specimen Dimensions in Millimeters

Appendix B. Specimen Manufacturing Data

Table 10. Manufacturing Data for the 25 Specimens and Test Order

Test order	Test point	Leveling	Fiber	Nylon	Start date MM/DD/YY	Width AVG (mm)	% diff Mean	Thickness AVG (mm)	% diff Mean	Weight (g)
9	1	2	2	1	08/01/16	15.13	-0.51%	3.03	-1.94%	12.85
20	1	2	2	1	08/02/16	15.21	0.04%	3.17	2.60%	12.98
5	1	2	2	1	08/02/16	15.20	-0.03%	3.14	1.63%	12.98
1	1	3	3	1	10/11/16	15.29	0.52%	3.10	0.22%	13.11
12	1	3	3	1	10/11/16	15.26	0.34%	3.08	-0.42%	13.32
15	2	5	4	1	05/02/16	15.21	0.02%	3.13	1.41%	13.72
17	2	5	4	1	05/02/16	15.27	0.39%	3.14	1.63%	13.79
21	2	5	4	1	05/02/16	15.30	0.59%	3.10	0.33%	13.72
10	2	5	4	1	05/02/16	15.32	0.74%	3.10	0.22%	13.46
24	2	5	4	1	05/02/16	15.20	-0.07%	3.03	-1.94%	13.50
13	3	1	1	1	07/11/16	15.19	-0.09%	3.06	-1.07%	13.04
3	3	1	1	1	07/02/16	15.10	-0.71%	3.00	-2.80%	12.65
18	3	2	2	1	07/13/16	15.05	-1.06%	3.00	-3.01%	11.12
4	3	2	2	1	07/13/16	15.20	-0.07%	3.02	-2.15%	12.79
6	3	2	2	1	07/18/16	15.07	-0.88%	3.02	-2.37%	12.86
23	4	3	3	1	11/01/16	15.26	0.32%	3.09	0.11%	13.24
25	4	3	3	1	11/02/16	15.30	0.59%	3.03	-1.83%	12.96
7	4	3	3	1	11/02/16	15.22	0.06%	3.09	0.01%	13.08
2	4	4	3	1	11/07/16	15.35	0.96%	3.03	-1.94%	12.87
11	4	4	3	1	11/07/16	15.23	0.15%	3.06	-1.07%	12.95
22	5	4	3	1	11/21/16	15.29	0.56%	3.20	3.46%	13.26
14	5	4	3	1	11/28/16	15.18	-0.18%	3.19	3.24%	13.21
16	5	4	3	1	11/29/16	15.16	-0.31%	3.19	3.24%	13.26
8	5	4	3	1	11/30/16	15.16	-0.34%	3.18	2.81%	13.22
19	5	4	3	1	12/01/16	15.06	-0.97%	3.09	0.11%	13.09

Appendix C. Calibration Samples Data

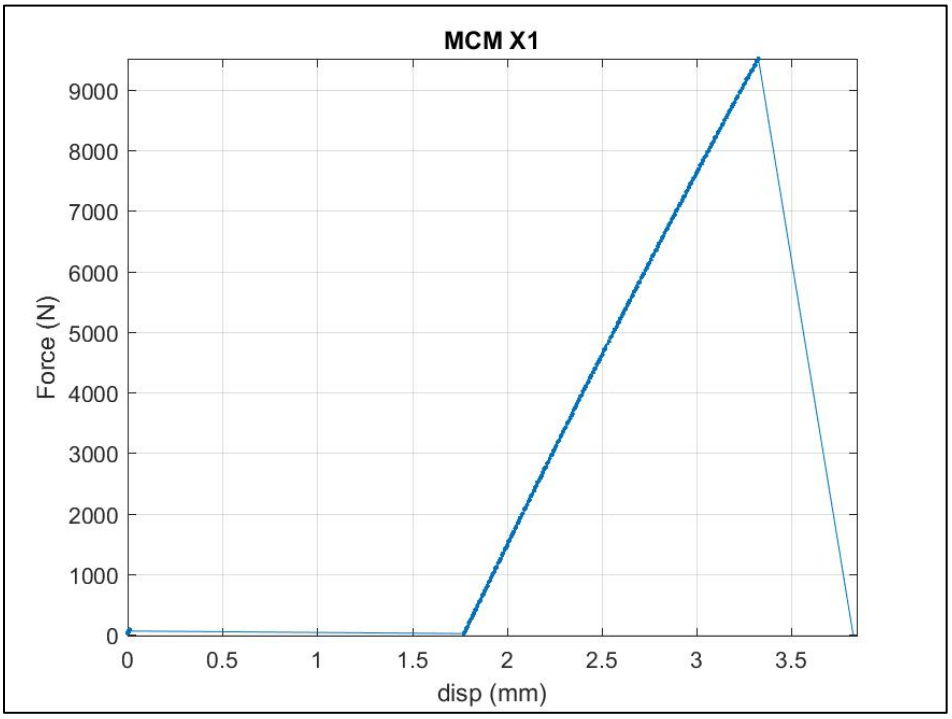

Figure 49. Force vesues Displacment for Calibraion Sample Number 1 With 500psi Grip Pressure and 50mm × 15mm × 1.5mm Fiberglass Tabs

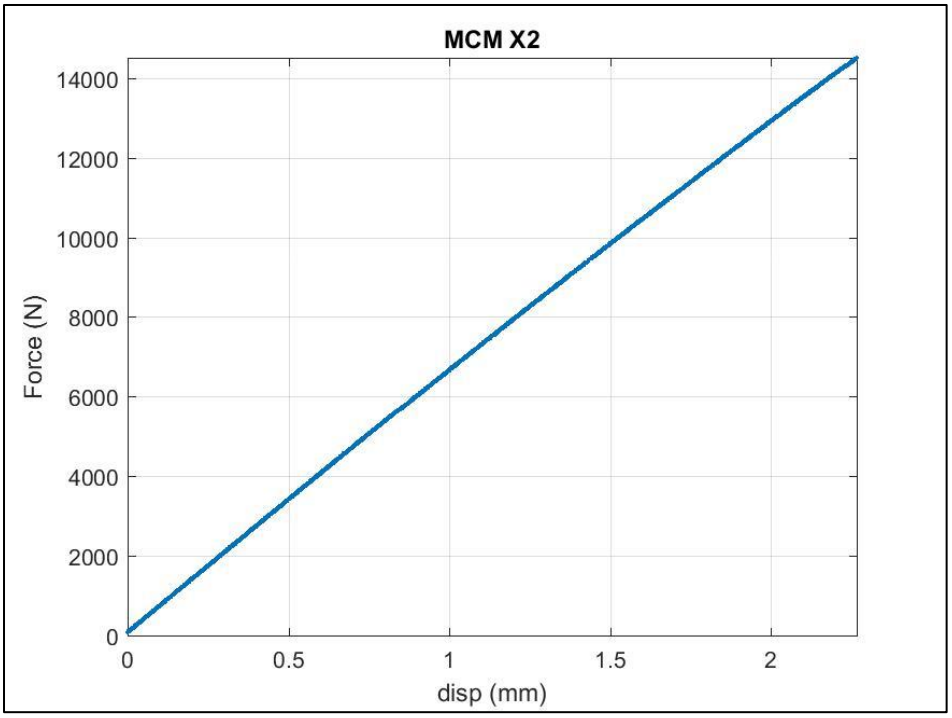

Figure 50. Force vesues Displacment for Calibraion Sample Number 2 With 600psi Grip Pressure and 50mm × 15mm × 1.5mm Fiberglass Tabs

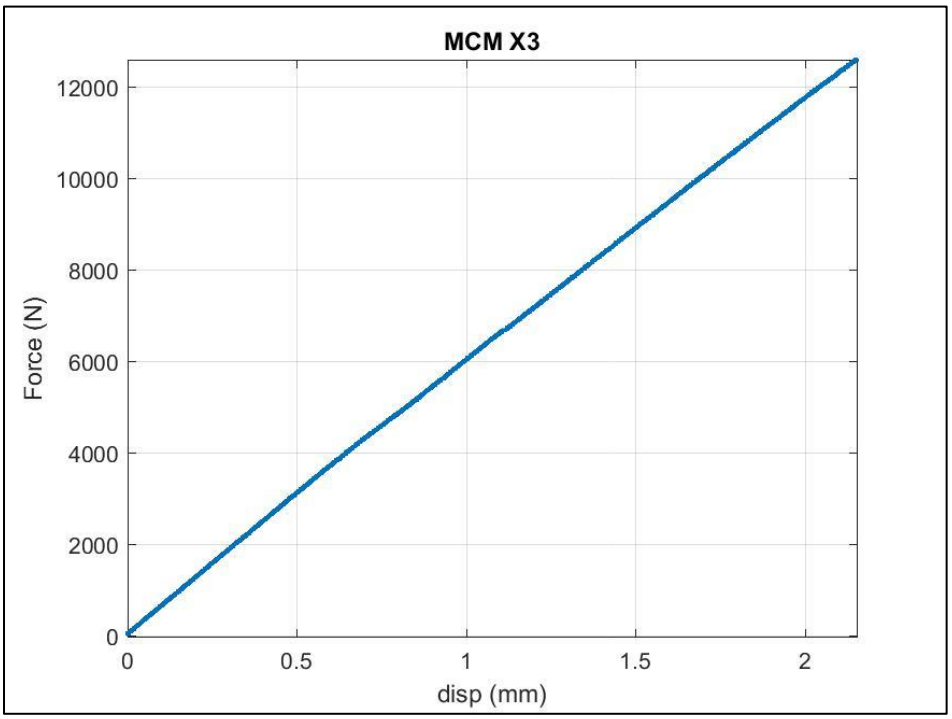

Figure 51. Force vesues Displacment for Calibraion Sample Number 3 With 600psi Grip Pressure and 50mm × 15mm × 1.5mm Fiberglass Tabs

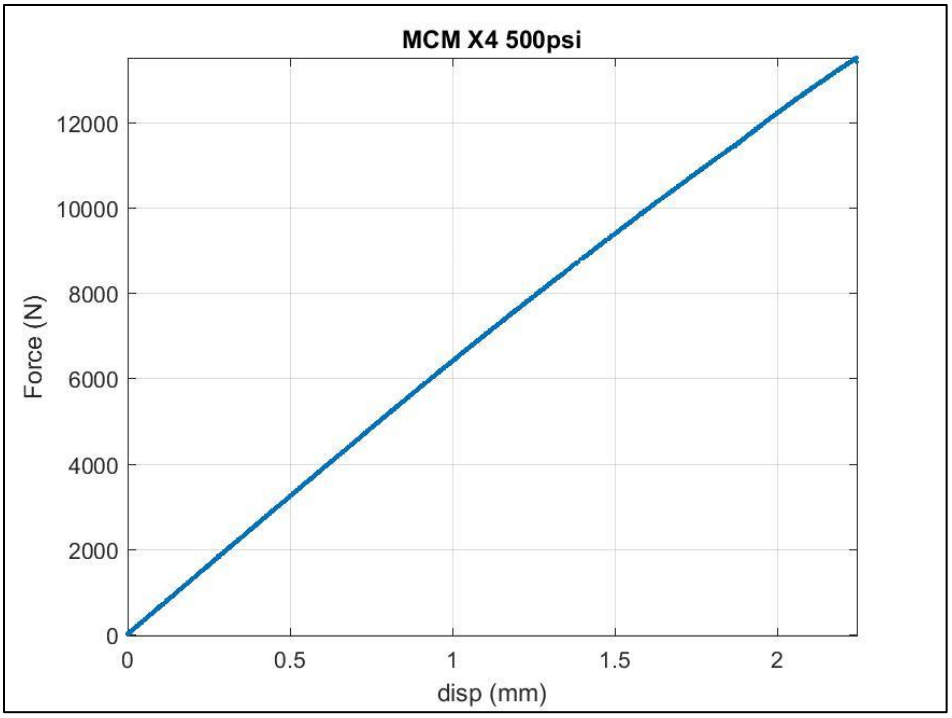

Figure 52. Force vesues Displacment for Calibraion Sample Number 4 With 500psi Grip Pressure and 50mm × 15mm × 1.5mm Fiberglass Tabs

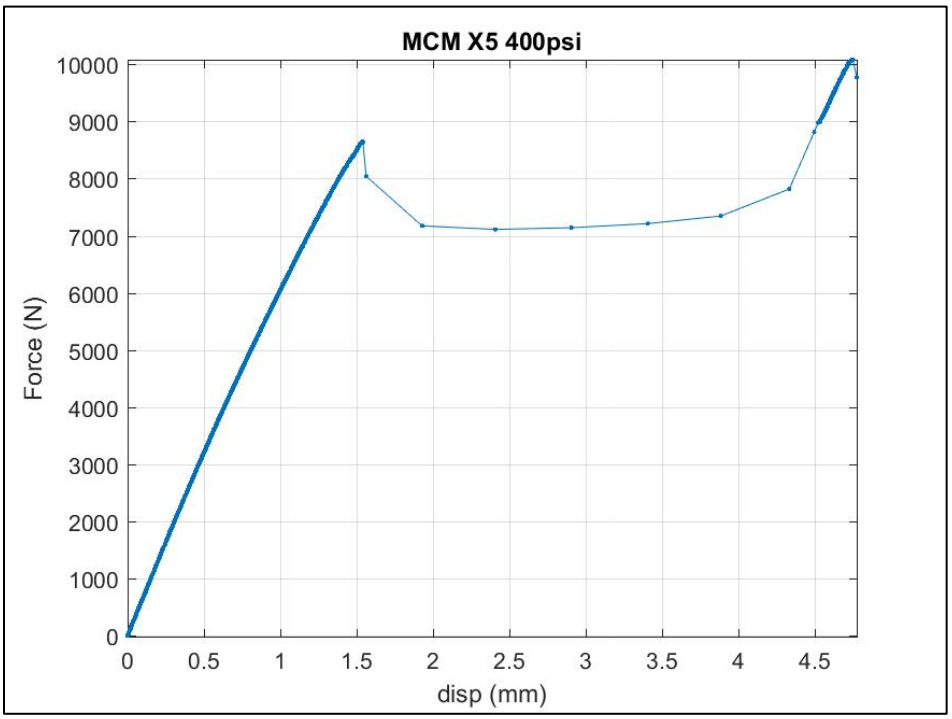

Figure 53. Force vesues Displacment for Calibraion Sample Number 5 With 400psi Grip Pressure and 50mm × 15mm × 1.5mm Fiberglass Tabs

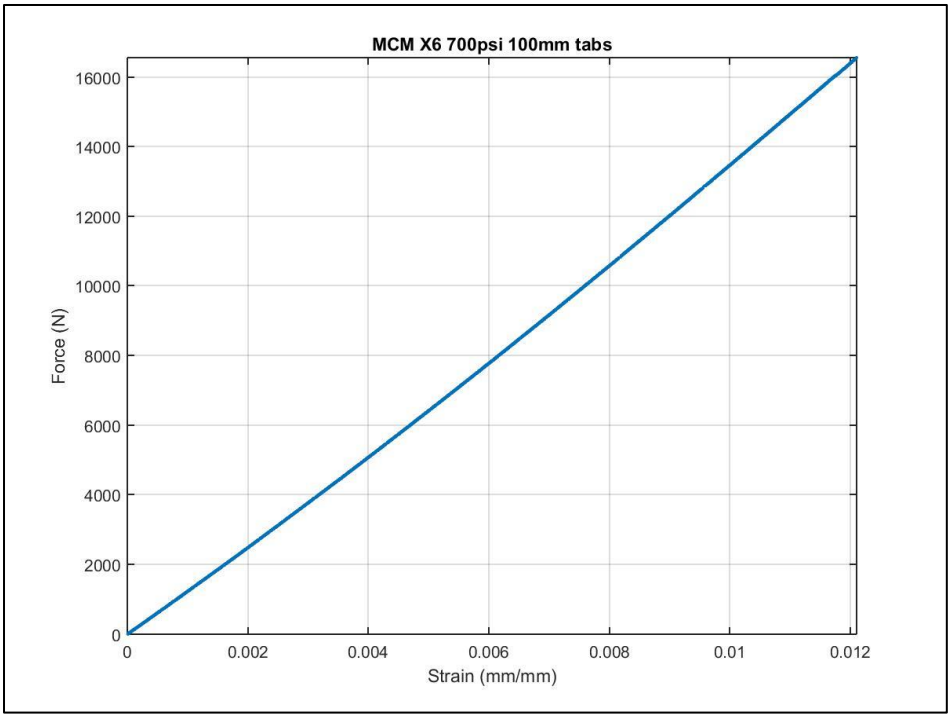

Figure 54. Force vesues Displacment for Calibraion Sample Number 6 With 700psi Grip Pressure and 100mm × 15mm × 1.5mm Fiberglass Tabs

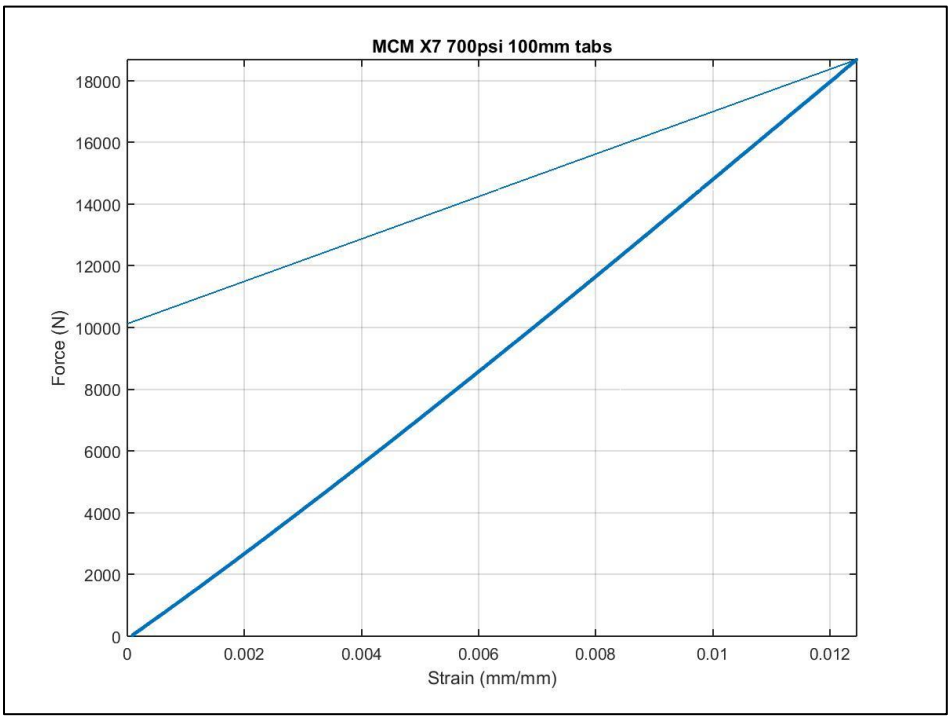

Figure 55. Force vesues Displacment for Calibraion Sample Number 7 With 700psi Grip Pressure and 100mm × 15mm × 1.5mm Fiberglass Tabs

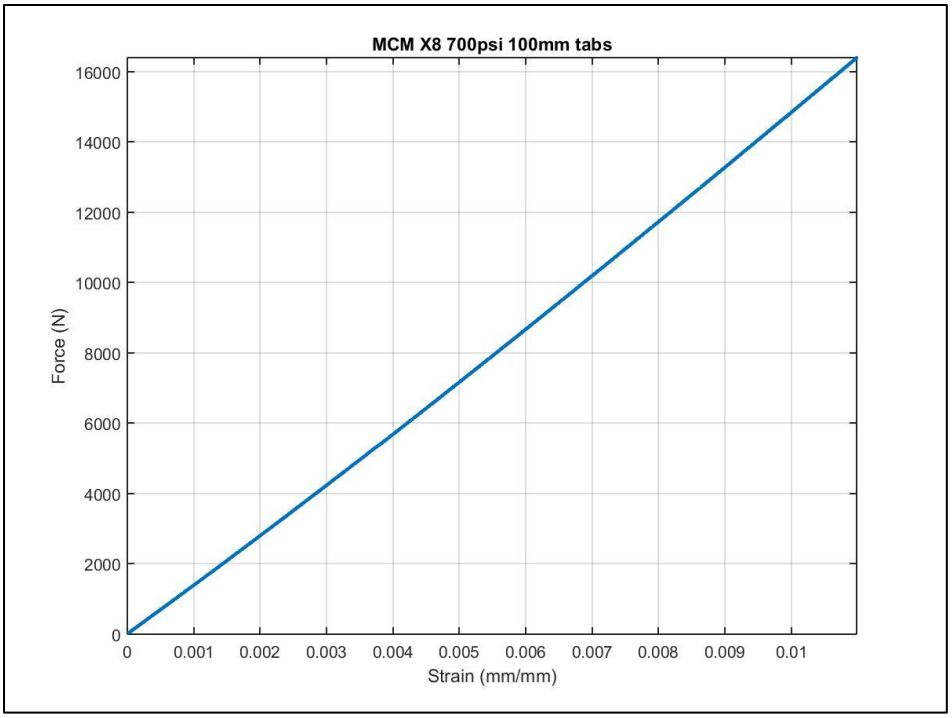

Figure 56. Force vesues Displacment for Calibraion Sample Number 8 With 700psi Grip Pressure and 100mm × 15mm × 1.5mm Fiberglass Tabs

Appendix D. Specimen Photography

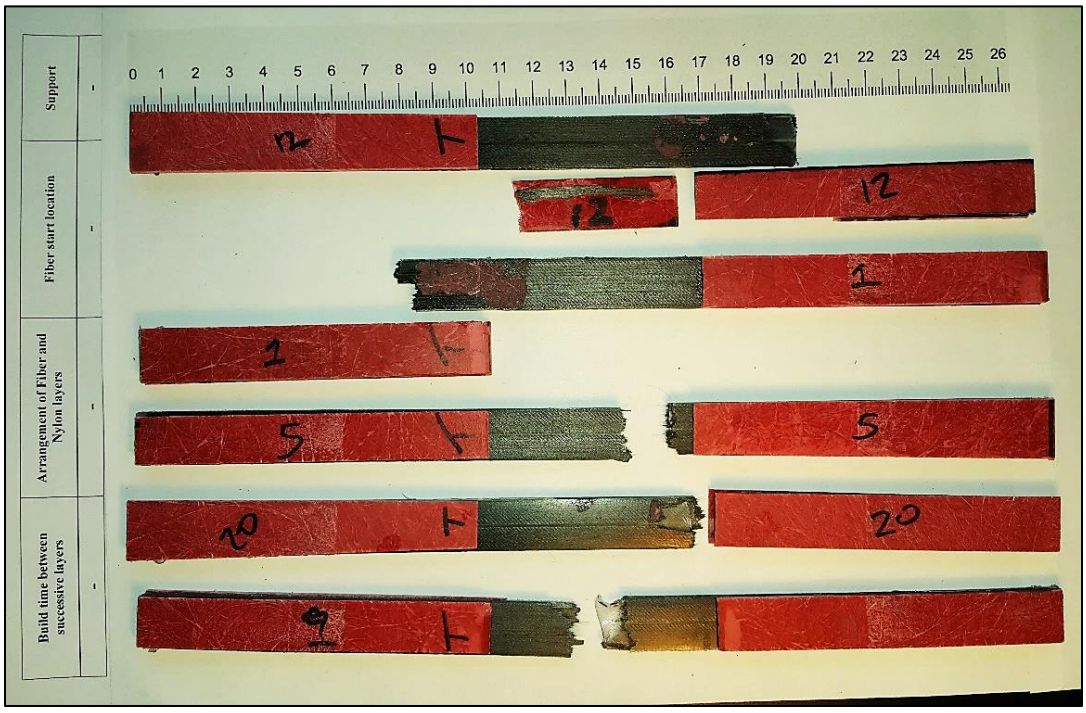

Figure 57. Test Point 1 After Testing

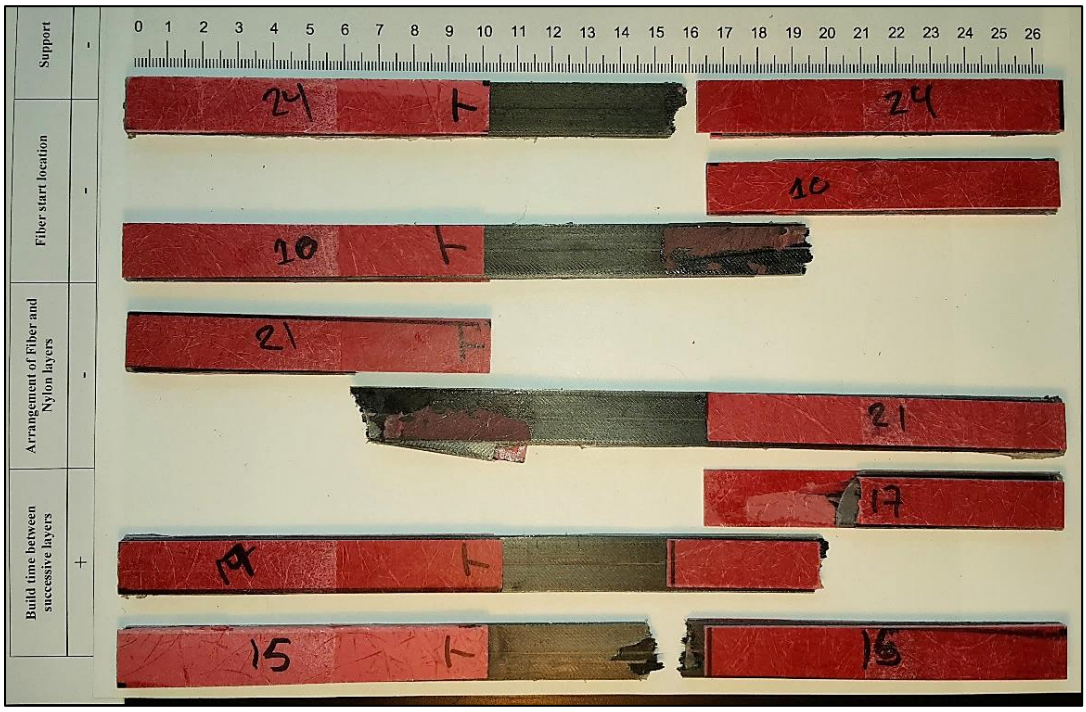

Figure 58. Test Point 2 After Testing

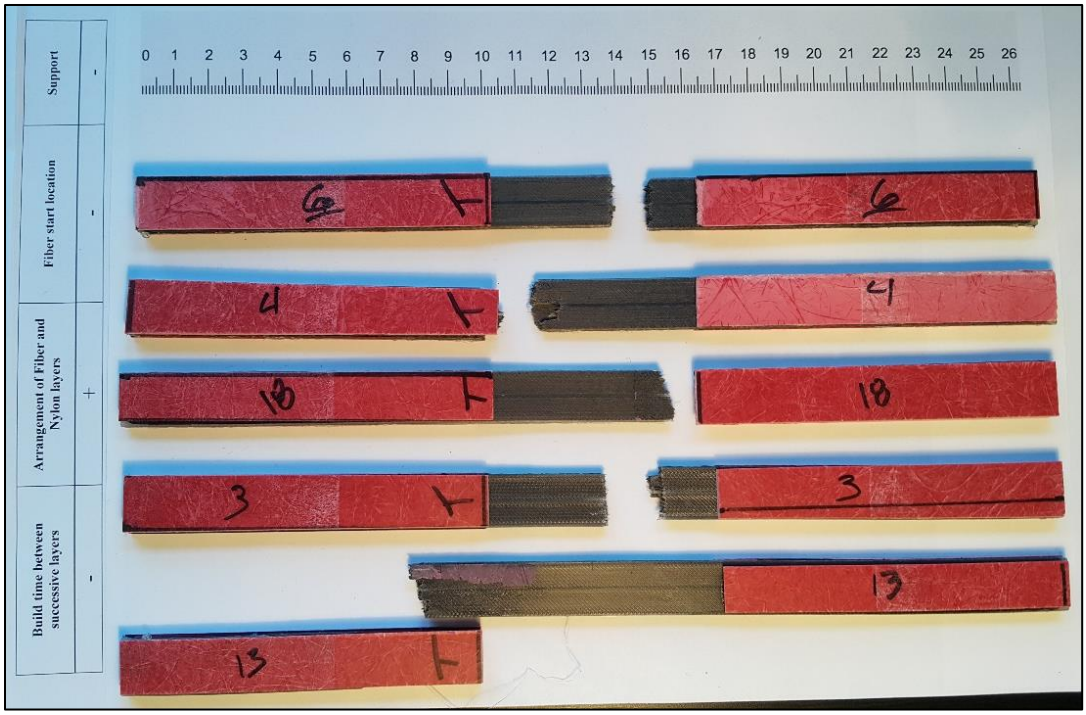

Figure 59. Test Point 3 After Testing

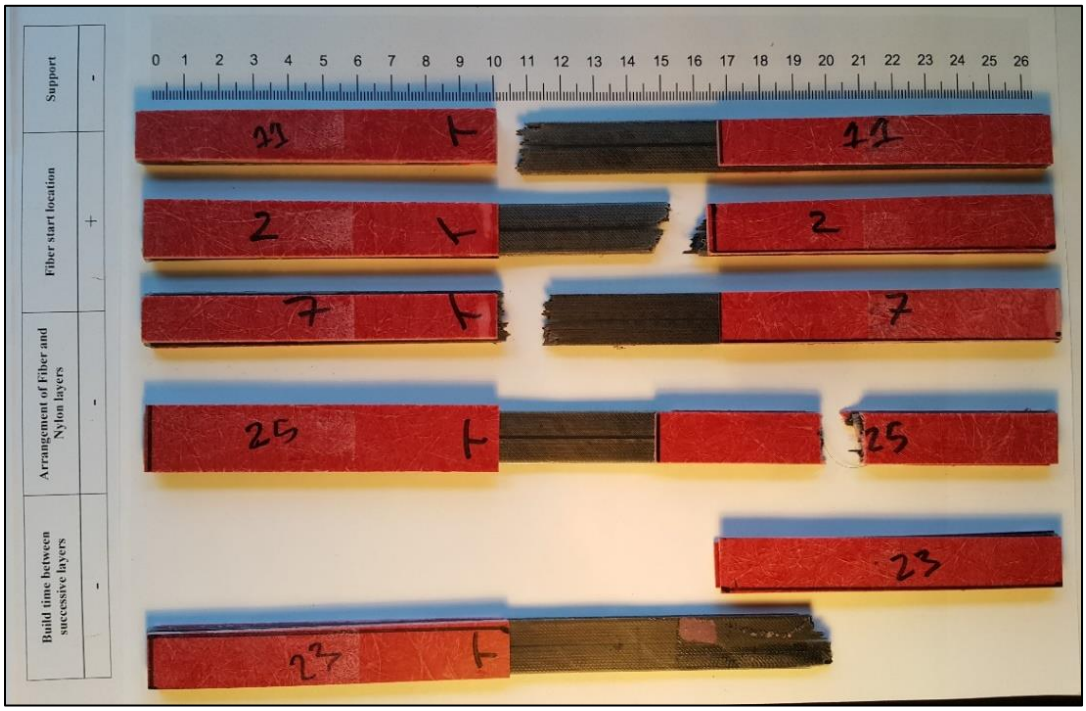

Figure 60. Test Point 4 After Testing

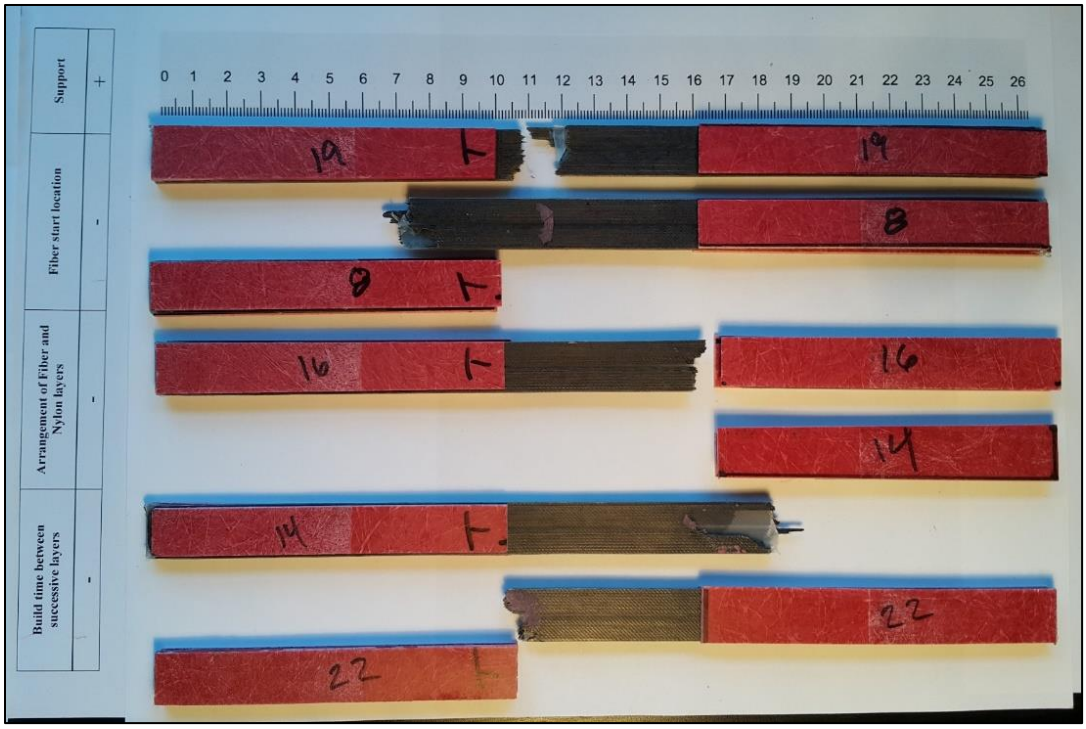

Figure 61. Test Point 5 After Testing

Bibliography

Anderson, M. J., & Whitcomb, P. J. (2007). *DOE Simplified: Practical Tools for Effective Experimentation*. *Productivity Press* (2nd ed.).

ASTM Standard D3039/D3039M. (2014). Standard Test Method for Tensile Properties of Polymer Matrix Composite Materials. *ASTM*.

Callister, W. D. (2007). *Materials Science and Engineering An Introduction*. John Wiley & Sons. Retrieved from https://books.google.com/books/about/Materials_Science_And_Engineering.html?id=cEmvx57kWRIC

Daniel, I. M., & Ishai, O. (2006). *Engineering mechanics of composite materials*. Oxford University Press. Retrieved from https://books.google.com/books/about/Engineering_Mechanics_of_Composite_Mater.html?id=x5S_QgAACAAJ

Eiger. (2016). Retrieved from https://www.eiger.io

Fisher, R. A. (1971). *The Design of Experiments*. *Hafner Publishing Company* (Eighth). New York: Hafner Publishing Company.

Gibson, I., Rosen, D., & Stucker, B. (2014). *Additive Manufacturing Technologies: 3D Printing, Rapid Prototyping, and Direct Digital Manufacturing* (Vol. 26). Springer. Retrieved from https://books.google.com/books?id=OPGbBQAAQBAJ&pgis=1

Holm, E. S. (2016). *Additive Manufacturing Process Parameter Effects on The Mechanical Properties of Fused Filament Fabrication Nylon*. *Transformation*. Air Force Institute of Technology, Air University.

Love, L. J., Kunc, V., Rios, O., Duty, C. E., Elliott, A. M., Post, B. K., Smith, R. J., Blue, C. A. (2014). The importance of carbon fiber to polymer additive manufacturing. *Journal of Materials Research*, *29*, 1893–1898.

MarkForged Inc. (2015). *MarkOne Mechanical Properties Data Sheet*. Retrieved from http://markforged.com

Masuelli, M. A. (2013). Introduction of Fibre-Reinforced Polymers − Polymers and Composites : Concepts , Properties and Processes. *The Technology Applied for Concrete Repair*, 3–40.

Stewart, P. F. (2005). Fractional Factorial Designs. *Encyclopedia of Biostatistics*. Retrieved from http://doi.wiley.com/10.1002/0470011815.b2a16025

REPORT DOCUMENTATION PAGE

Form Approved
OMB No. 0704-0188

1. REPORT DATE *(DD-MM-YYYY)*	2. REPORT TYPE	3. DATES COVERED *(From - To)*
14 September 2017	Master's Thesis	Sept 2015 – Sept 2017

4. TITLE AND SUBTITLE

Effect of Fused Filament Fabrication Process Parameters on the Mechanical Properties of Carbon Fiber Reinforced Polymers

5a. CONTRACT NUMBER

5b. GRANT NUMBER

5c. PROGRAM ELEMENT NUMBER

6. AUTHOR(S)

Alwabel, Abdulrahman, S, 1LT, RSAF

5d. PROJECT NUMBER

5e. TASK NUMBER

5f. WORK UNIT NUMBER

7. PERFORMING ORGANIZATION NAME(S) AND ADDRESS(ES)

Air Force Institute of Technology
Graduate School of Engineering and Management (AFIT/EN)
2950 Hobson Way
Wright-Patterson AFB OH 45433-7765

8. PERFORMING ORGANIZATION REPORT NUMBER

AFIT-ENV-MS-17-S-046

9. SPONSORING / MONITORING AGENCY NAME(S) AND ADDRESS(ES)

Office of the Secretary of Defense
ATTN: Catherine Warner
1700 Defense Pentagon
Washington D.C., 20301

703) 697-7247
Catherine.Warner@osd.mil

10. SPONSOR/MONITOR'S ACRONYM(S)

OSD DOT&E

11. SPONSOR/MONITOR'S REPORT NUMBER(S)

12. DISTRIBUTION / AVAILABILITY STATEMENT

DISTRIBUTION STATEMENT A. APPROVED FOR PUBLIC RELEASE; DISTRIBUTION UNLIMITED.

13. SUPPLEMENTARY NOTES

This material is declared a work of the U.S. Government and is not subject to copyright protection in the United States.

14. ABSTRACT

Carbon fiber reinforced polymer manufactured using additive manufacturing process is relatively a new process. The ability to predict the mechanical properties of these parts with high confidence will spread the use of these high-strength materials in more applications. The purpose of this research was to determine the effect of the build time between successive layers, arrangement of fiber and nylon layers, fiber start location, and the use of support material on the mechanical properties CFRP produced by additive manufacturing process using the MarkForged (MarkOne) 3D printer. A design of experiment (DOE) we preformed to develop a mathematical model describing the functional relationship between the tensile strength of additively manufactured composites and the selected additive manufacturing build process parameters. Testing was performed in accordance with ASTM standard D3039 using the 25 manufactured specimens. The mechanical properties were measured in the experiment were tensile strength, and tensile stress. A liner regression analysis was preformed to determine the relation between the ultimate tensile strength and the main level interactions of the four build parameters. The results showed a significant positive relation longer the build time between successive layers, and negative relation with the other fiber and nylon layer arrangement. However, the two other build parameters showed negative, but not significant results.

15. SUBJECT TERMS

Carbon Fiber Reinforced Plastic, Additive manufacturing.

16. SECURITY CLASSIFICATION OF:			17. LIMITATION OF ABSTRACT	18. NUMBER OF PAGES	19a. NAME OF RESPONSIBLE PERSON
a. REPORT	b. ABSTRACT	c. THIS PAGE			Maj Jason Freels AFIT/ENV)
U	U	U	UU	74	19b. TELEPHONE NUMBER *(include area code)* (937)255-3636 x4676 Jason.freels@afit.edu

Standard Form 298 (Rev. 8-98)
Prescribed by ANSI Std. Z39.18